Investigating the role of urban vegetation alongside other environmental variables in shaping *Aedes albopictus* presence and abundance in Montpellier, France

Colombine Bartholomée[1*], Paul Taconet[1], Mathilde Mercat[1], Coralie Grail[1], Emilie Bouhsira[2], Florence Fournet[1] and Nicolas Moiroux[1*]

[1] MIVEGEC, Univ. Montpellier, CNRS, IRD, Montpellier, France

[2] InTheres, Univ. Toulouse, INRAE, ENVT, Toulouse, France

Corresponding authors

E-mail: colombine.bartholomee@ird.fr (CB), nicolas.moiroux@ird.fr (NM)

Abstract

Urban greening helps address urbanization challenges and provides health benefits, but it may also favor mosquito species, vectors of pathogens causing human diseases. This study examines the relationship between urban vegetation and the presence and abundance of *Aedes albopictus* in Montpellier, the second greenest city of France, while accounting for meteorology, microclimate, air quality, human socio-demography, and landscape.

From May to October 2023, adult mosquitoes were collected monthly in urban parks, residential areas, and the impervious city center using BG-Pro traps with odor and CO_2 attractants. Microclimate data were recorded on-site. Vegetation, land cover, meteorological, air quality, and human demographic data were gathered from open-access databases. *Ae. albopictus* presence and abundance were analysed according to environmental variables taken at different time lags and spatial distances using a two-stage modeling approach: bivariate analyses using generalized linear mixed models were conducted to select variables for inclusion in a multivariate random forest model, aiming to identify the factors that best explain *Ae. albopictus* presence and abundance.

While urban vegetation had a limited effect on *Ae. albopictus* presence, number of patches and the percentage of area covered by low vegetation were among the most important predictors of abundance. The main predictors for presence were minimum hourly temperature (24h-48h before sampling), minimum atmospheric pressure during sampling, and the weekly cumulated rainfall recorded six weeks before sampling. The most important predictors of abundance were maximum hourly temperatures during sampling, cumulated growing degree days (GDD) during two weeks preceding sampling and the length and patch

size of roads. To our knowledge, this is the first study examining urban vegetation's influence on *Ae. albopictus* in France, offering insights for urban planning and suggesting further research on vegetation's role in mosquito-borne disease transmission, particularly in the context of increasing dengue incidence in Europe.

Author summary

Urban greening is often promoted as a solution to the challenges posed by increasing urbanization, offering numerous environmental and societal benefits. However, it may also create favorable conditions for mosquito vector species such as *Aedes albopictus*. Only two studies in Europe—both conducted in Italy—have investigated the impact of urban vegetation on the presence and abundance of *Ae. albopictus*. This study explores this relationship in Montpellier, the second greenest city in France, while considering meteorology, microclimate, air quality, human socio-demographic factors, and landscape characteristics. Using a two-stage modeling approach, we first performed bivariate analyses with generalized linear mixed models to select relevant variables, which were then integrated into a multivariate random forest model to identify the key predictors of *Ae. albopictus* presence and abundance. Our results indicate that urban vegetation does not significantly influence *Ae. albopictus* presence but is among the most important predictors of its abundance. These findings provide valuable insights for urban planning and highlight the need for further research on the role of vegetation in mosquito-borne disease transmission.

Introduction

According to Hussain and Imitiaz [1], urbanisation is a complex, dynamic, and evolving social process that drives the emergence and growth of cities. It occurs unevenly across time and space, with disparities between continents and countries. Cities are mosaics of heterogeneous patches of diverse ecosystems with multiple interfaces [2]. Urbanisation can improve public health by enhancing living standards for citizens [3]. However, it also results in habitat loss and fragmentation, leading to a decline in biodiversity, as observed in China for birds species diversity [4]. Urbanisation also exacerbates air pollution [5], contributing to human health issues [6]. Moreover, social disparities and the lack of contact with nature favour mental health disorders [7]. Finally, the expansion of asphalt-covered areas that absorb energy during the day and release it as heat at night amplifies the urban heat island (UHI) effect [8], worsening its impact on human health [9].

Nature-Based Solutions (NBS), such as urban greening, are promoted to achieve the 11th Sustainable Development Goal: "to make cities and human settlements inclusive, safe, resilient, and sustainable" [10]. NBS also support the 12th target of the COP 15 Biodiversity Plan for Life on Earth, aiming to "enhance green spaces and urban planning for human well-being and biodiversity" [11], and align with the sustainability goals of the European Green Deal [12]. Urban greening involves deliberately integrating vegetation into urban areas (13), encompassing initiatives such as soil de-imperviousness, developing green and blue infrastructures, conserving urban green spaces (UGS), and promoting urban agriculture. UGS provide cultural and regular ecosystem services [13]. They help mitigate the UHI effect [14,15], and contribute to improving mental health [16]. Effective management of UGS can

help sequester carbon dioxide [17] through tree plantations and enhance animal biodiversity by increasing the presence of indigenous vegetation [18].

Urban greening may also have negative side effects. It can increase pollen allergies [19] and attract agricultural pests like tree moths [20]. UGS increase human-wildlife interactions, raising the risk of zoonotic [21] and arthropod-borne diseases [22], as shown for the Lyme disease pathogen (*Borrelia burgdorferi*) transmitted by ticks in urban parks across Europe [23]. In Europe, while numerous studies have explored the relationship between UGS and tick populations, the relationship between urban greening and mosquitoes is less documented [24], with only one study on *Culex pipiens* in the Netherlands [25] and two studies on the tiger mosquito *Aedes albopictus* in Italy [26,27]. As shown in the scoping review by Mercat *et al* (2025) [24], the effects of urban green infrastructures (UGIs) on mosquito populations are highly dependent on the vector system studied and the environmental context. Urban greening is a dynamic process, and its environmental changes may take time to manifest [28]. While it can create favorable conditions for vectors and increase human-vector interactions, it may also promote the establishment of predators that could regulate vector populations.

Ae. albopictus is an invasive mosquito in Europe. It is native to Southeast Asia and a vector of several infectious agents, including the dengue virus (DENV), chikungunya virus (CHIKV), and Zika virus. The species adapted to antropogenic environments [29], including urban areas, using natural and artificial breeding sites. It can survive extreme conditions through egg diapause [30]. Its abundance is influenced by environmental factors such as weather [31], microclimate [32], and landscape features [33]. Urban vegetation may favour *Ae. albopictus* by creating cooler and more humid microclimates during warm season [34], facilitating access to sugar meals, providing natural resting sites [35], and attracting blood sources (humans and animals). In France, since its first detection in 2004 [36], *Ae. albopictus* spreads to 78 of 96

metropolitan France's departments by 2024, including all departments in the Occitanie region, where it has been linked to several autochthonous arboviral disease clusters since 2014.

The Occitanie region is actively pursuing urban greening projects in its two largest cities, Toulouse and Montpellier, including plans to plant 150 000 trees. As Occitanie is a hotspot for both arboviral diseases and urban greening, it is crucial to assess the impact of these greening initiatives on *Ae. albopictus* population dynamics. With the goal to guide future research to improve the design and planning of urban green spaces, this study aims to evaluate the influence of urban vegetation in Montpellier in 2023 on the presence and abundance of *Ae. albopictus* females, using an explanatory approach taking into account land cover, microclimate, meteorology, air quality, and socio-demographics.

Material and methods

Mosquito sampling and study areas

Study areas

Montpellier is a city of 300 000 inhabitants located in the Occitanie region in southern France (Fig 1). The city has a Mediterranean climate with an average annual temperature of 15°C and an average annual precipitation of 739 mm [37]. The city features more than 10% of vegetated areas within densely urbanized areas. It ranks among the top three greenest cities in metropolitan France [38]. The study was conducted in nine areas belonging to three different environments: two urban parks (PRK), three residential neighborhoods (RES), and four densely built impervious areas (IMP) (Fig 1). Urban parks (Botanical Garden (PRK-BOT), and Park of

Aiguelongue (PRK-AGL)) and residential neighborhoods (Lemasson (RES-LEM), Aiguerelles (RES-AGR), and Soulas (RES-SOUL)) were vegetated. The densely built impervious areas included two areas with some vegetation (Saint Charles University (IMP-SCU) and Acapulco Hotel (IMP-ACA)) and two with little to no vegetation (Buisson Bertrand Institute (IMP-BBI) and Diderot School (IMP-DID)) (Fig 1). Detailed descriptions of study areas are provided in S1 Table, and images of study areas in S1 Fig. The minimum distance between study areas was 115 m. Although *Aedes* mosquitoes can disperse from 75 m [39] to 290 m [40] in urban areas over 8 days, we treated the study areas as independent units due to impervious roads between them, that are known to limit mosquito dispersal [41,42].

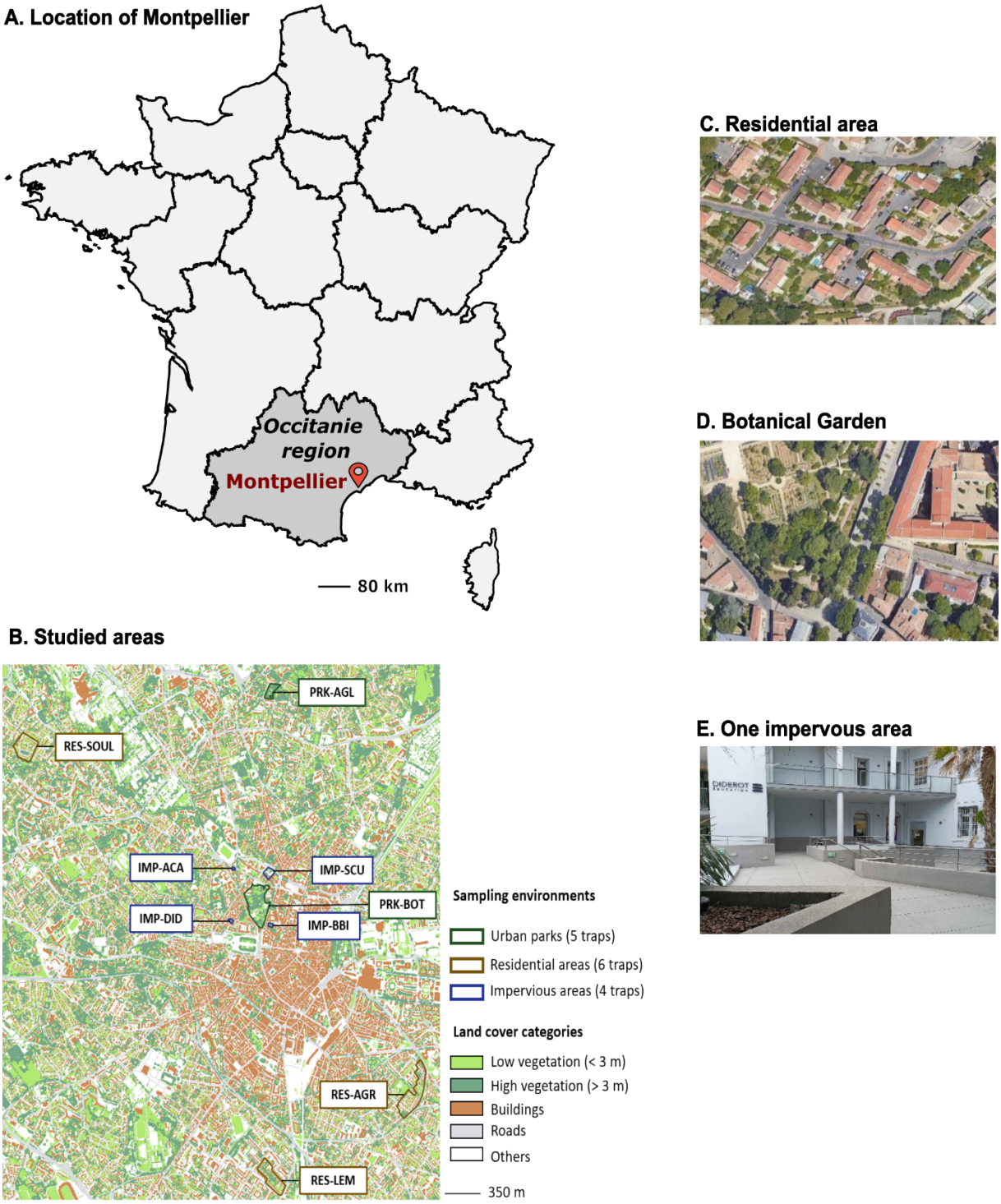

Fig 1: **Study areas**. Fig 1A and 1B show the location of Montpellier in France (map from OpenStreetMap) and the land cover map of Montpellier with the study areas, respectively. Sampling environments are shown in the legend of Fig 1B, delineating urban parks, residential areas, and impervious built-up areas (boundaries from Montpellier Open Data). Land cover categories are shown in the legend of Fig 1B. Fig 1C, 1D, and 1E show a residential area, the

southern part of the Botanical Garden (PRK-BOT), the Bouisson Bertrand Institute (IMP-BBI) and the Diderot School (IMP-DID) respectively.

Mosquito sampling

Adult mosquitoes were captured using BG-Pro traps (BioGents, Regensburg, Germany) modified according to L'Ambert *et al* [43], each equipped with a BG lure—synthetic human odor mimic—and a daily replenished carbon dioxide source made from yeast, sugar, and water (S1 Fig). Two BG-Pro traps were installed in each residential area (RES-LEM, RES-AGR, RES-SOUL), and in the park of Aiguelongue (PRK-AGL). Due to their smaller size (S1 Table), only one BG-Pro trap was deployed in each of the impervious built areas (IMP-ACA, IMP-BBI, IMP-DID and IMP-SCU). Because of its larger size (S1 Table), three BG-Pro traps were deployed in the Botanical Garden (PRK-BOT).

Traps were placed in shaded, wind-sheltered sites at a height of one meter. Therefore, 15 sites were sampled: five in the two urban parks, six in the three residential areas, and four in impervious built areas. Every trap was separated by a minimum distance of 50 m to prevent interferences [44]. However, due to accessibility constraints, the two traps in RES-SOUL were placed 22 m apart.

Every sampling session occurred for 48 hours each month from May to October 2023. Mosquitoes were retrieved every morning, transported at 4°C to the laboratory (MIVEGEC laboratory, IRD regional delegation, Montpellier), and stored at -20°C. Mosquito individuals were then counted, sorted by sex, and morphologically identified using the multicriteria key MosKeyTool [45]. These data are available on GBIF [46].

Environmental data collection and preparation

To assess the impact of urban vegetation on the presence and abundance of *Ae. albopictus*, it was essential to consider all factors that may influence its population dynamics. For this task, we adapted the conceptual model of human-*Anopheles* contact by Moiroux (2012) [47] to the case of *Ae. albopictus*. Based on a literature review, we documented and hypothesised known or potential predictors and their pathways to mosquito abundance [48]. This model guided the selection of environmental data to be collected as described below.

Fine-scale vegetation and land cover data

The vegetation data were extracted from the fine-scale vegetation dataset of Montpellier created in 2019 by Montpellier Mediterranée Métropole (S2 Table). The vegetation data were categorised into low vegetation (< 3 metres in height) and high vegetation (> 3 metres in height). In addition, a land cover map (Fig 2B) was generated by combining these vegetation data with data from two open access databases: the Urban Atlas of the Copernicus European Union's space program component and the French national database of Buildings (S2 Table). The produced dataset included five categories: buildings, roads, low vegetation, high vegetation, and "others" (that included railways, pathways, industrial areas, and sports facilities). For each land cover category, the percentage of cover, total edge length, and average patch size were calculated in buffer zones with radii of 20 m, 50 m, 100 m, and 250 m around each trap location. For vegetation categories, the number of patches was also extracted for each of the four buffer zones. The landscape diversity (Shannon index) was calculated for all buffer zones (S2 Table). Buffer sizes were chosen according to previous works investigating the effect of urban vegetation [27,49] on the dispersal of *Ae. albopictus* [40]. Table S3 provides the land cover variable values for each trap and buffer radii.

Microclimatic, meteorological and air quality data

We continuously collected hourly temperature and relative humidity near each trap using Hygro Button data loggers from May to October 2023. The minimum (lowest recorded value), maximum (highest recorded value), and mean temperatures, as well as relative humidity, were calculated per 24-hour periods from 48h before the start of each sampling session to its end (S2 Table).

Hourly temperature and rainfall data were obtained from the Observatoire Départemental de l'Eau et de l'Environnement (ODEE) station located at Château d'Ô in the north-west of Montpellier (S2 Table). Precipitations were recorded per 24-hour periods before and during sampling sessions as for datalogger data. Relative humidity and wind speed data were recorded every three hours from the Frejorgues airport station (belonging to the Meteo France national meteorology agency network) (S2 Table). Growing Degree Days (GDD), a known predictor of mosquito development, were calculated from daily mean temperatures above 11°C, as this was shown to be the annual mean temperature limit for the establishment of *Ae. albopictus* populations [50]. Temperatures above this level are conducive to mosquito development. All weather data were aggregated for the sampling week and each of the six weeks before sampling. Rainfall data and GDD were summed, while temperature, humidity, and wind speed were averaged.

Atmospheric pressure can influence insects' flight [51] and locomotor activity [52], as shown in *Drosophila* and beetles. Haufe, in 1954 [53], demonstrated that variations in atmospheric pressure can affect the flight activity of *Aedes aegypti.* To evaluate the effect of daily atmospheric pressure on *Ae. albopictus*, the minimum (lowest recorded value), maximum (highest recorded value), and mean atmospheric pressure, measured every three hours at the

Frejorgues airport station, were extracted per 24-hours periods before and during sampling sessions. The daily mean atmospheric pressure difference between two consecutive days was calculated per 24-hours periods before and during sampling sessions. S2 Fig depicts the temporal evolution of these meteorological variables (temperature, rainfall, wind speed, relative humidity, and atmospheric pressure).

Air pollution can influence insect behaviour and abundance. Particulate matter (PM10, PM2.5) affects pollinator orientation and reduces honeybee fitness [54]. Ozone (O3) impairs honeybee antenna perception [54] and lowers pollinator abundance [55]. Nitrogen monoxide (NO) and nitrogen dioxide (NO2) reduce the pollinator performance [56]. To evaluate the effect of air quality data on *Ae. albopictus*, for each trap location, we collected daily concentrations of nitrogen monoxide (NO), nitrogen dioxide (NO2), particulate matter (of diameter less than 10 (PM10) and 2.5 µm (PM2.5)), and ozone (O3) from the closest station of the Atmo Occitanie air quality observatory (S2 Table). Data were averaged weekly for up to 6 weeks, as for relative humidity, wind speed and temperatures, prior to each sampling session.

Social and demographic data

Socioeconomic factors such as low living standards [57], aging or degrading infrastructure [58], and population densities [59] can influence mosquito presence. Data on infrastructure age and number of low-income households were obtained as a 200m spatial resolution grid from the Filosofi database of the French Institut National de la Statistique et des Etudes Economiques (INSEE). Values of the grid cells that intersect trap locations were retrieved. Population density data were sourced from the Montpellier fine-scale population dataset,

created in 2016 by the Languedoc-Roussillon Geographic Information System (SIG-LR) (S2 Table) and aggregated within the same four buffer zones used for land cover data.

Statistical analyses of the presence and abundance of female *Ae. albopictus*

To study the relationships between the presence and the abundance of female *Ae. albopictus* and environmental conditions, we analysed the data using a hurdle modeling approach, i.e. considering the data responding to two distinguished processes: one causing zero vs. non-zero (« presence » models) and one causing positive counts of females (« abundance » models). This approach is justified because determinants of mosquito presence are expected to be different than abundance ones [60].

For both presence and abundance analysis, we adopt a two-stage analysis method as described by Taconet *et al* [61]. The first step involves bivariate analyses using Generalized Linear Mixed Models (GLMMs), followed by the second step, a multivariate analysis employing an interpretable machine learning method based on random forest models [62]. The bivariate analyses aimed to improve our understanding of (i) the time-lagged effects of meteorological and air quality variables, (ii) the impact of atmospheric pressure and microclimate on the tiger mosquito, (iii) land cover-scale effects, (iv) effects of socio-economic and demographic variables, and (iv) to identify and select key variables for multivariate analysis. The multivariate analysis aimed to identify the most impactful determinants of the presence and abundance of *Ae. albopictus* and the shape of their association while considering potentially complex (e.g. non-linear) associations and interactions between variables, with the overall aim

of assessing more precisely the impact of urban vegetation. The modeling workflow is summarised in S3 Fig.

Bivariate analysis using GLMMs

Every explanatory variable was tested using a GLMM with crossed random intercepts for trap location, with sites nested within the sampling area, and for the sampling session. We fitted binomial and zero-truncated negative binomial models to presence/absence and positive counts data, respectively. Marginal R^2, representing the proportion of variance explained by the fixed effects excluding the contribution of random intercepts [63], was calculated and used for interpretation. Time-lagged effects of meteorological and air quality variables were interpreted using cross-correlation maps (CCMs) [64] of marginal R^2 adjusted for the direction (+/-) of the relationship.

Multivariate analysis using random forests

The results of the bivariate analyses were used to select the variables to be included in the multivariate analysis. First, we excluded variables poorly correlated with the response variables ($p > 0.2$). For each meteorological, microclimatic, air quality, land cover, and demographic variable, we retained the time lag or radii with the higher marginal R^2. Multicollinearity was addressed using Pearson's correlation coefficient with a threshold of 0.7. Then, based on empirical knowledge, an initial selection of correlated variables was made. Other collinear covariates were removed until the Variance Inflation Factor (VIF) of the remaining variables was below three [65] (S3 Fig). Binary classification random forests (RFs) and regression classification RFs were generated for the presence and abundance models, respectively. To improve model efficiency and reduce the number of explanatory variables,

recursive feature elimination was performed for each model [66]. To account for spatial and temporal autocorrelation, sampling variables (trap location, sampling day, and sampling session) were included. For each set of hyperparameters and to assess the predictive power of each model, both a spatial and temporal cross-validation framework [67] was used, taking into account the potential spatial and temporal autocorrelation in the data. Spatial cross-validation (leave-area-out) involved training the model recursively on data from eight out of the nine sampled areas, testing it with data from the remaining area, and finally averaging the performance metric for the nine areas [61]. The temporal cross-validation (leave-sampling-session-out) involved training the model recursively on data from six out of the seven sampling sessions and testing it with data from the remaining session. The performance metrics selected were the Area Under the Curve (AUC) for the presence models [68] and the Mean Absolute Error (MAE) for the abundance models. The model results were interpreted using Variable Importance Plots (VIPs) [62] and Partial Dependence Plots (PDPs) [69]. Residual spatial autocorrelation was assessed for each model.

Softwares used

The R version 4.2.3 programming language [70] was used. The land cover map creation and landscape metrics calculation involved the use of the ‘sf’ [71], ‘raster’ [72], ‘fasterize’ [73], and ‘landscapemetrics’ [74] packages. GLMMs were fitted using the ‘glmmTMB’ package [75]. Marginal R^2 was calculated using the 'performance' package [76]. The ‘correlation’ package was used to evaluate multicollinearity [77]. Multivariate analyses were performed using the ‘caret’ [78] and ‘ranger’ [79] packages. The ‘CAST’ package [80] was used for the cross-validation and the interpretation plots were performed using the ‘iml’ [81], the ‘pdp’ [82], the ‘MLmetrics’ [83], the ‘precrec’ [84] and the ‘patchwork’ [85] packages. The package ‘spatialRF’

320 [86] was used to assess spatial autocorrelation. All scripts are available on Software Heritage
321 [87].
322

323 Results

324

325 Entomological data

326 A total of 2344 mosquitoes were collected, predominantly *Ae. albopictus* (85.66%, N=2008),
327 with smaller proportions of *Culex pipiens* (13.91%, N=326), *Culiseta longiareolata* (0.39%,
328 N=9), and *Culiseta annulata* (0.04%, N=1). Among 2008 collected *Ae. albopictus*, there were
329 1106 females (55.08%) and 902 males (44.92%). The mean density of female *Ae. albopictus*
330 was 3.83 mosquitoes/trap/24h (SE = 1.97) in urban parks, 3.31 mosquitoes/trap/24h (SE =
331 1.65) in residential areas, and 1.99 mosquitoes/trap/24h (SE = 1.08) in impervious built-up
332 areas (Table 1). Mean mosquito densities (mosquitoes/trap/24 h), stratified by sampling
333 environment (or sampling areas), are presented in Table 1 (or S4 Table). The temporal
334 distribution of *Ae. albopictus* (S4 Fig) exhibited a bimodal pattern, with an initial emergence
335 in May, a primary peak in late June, and a secondary, smaller peak in late August.
336

337 **Table 1: Mosquito density/trap/24h by species and sex in the three different sampling**
338 **environments.**

339

Environment	Mosquito female /trap/24h (± SE)	Mosquito male /trap/24h (± SE)	*Ae. albopictus* female /trap/24h (± SE)	*Ae. albopictus* male /trap/24h (± SE)	*Cx. pipiens* female /trap/24h (± SE)	*Cx. pipiens* male /trap/24h (± SE)	*Cu. longiareolata* female /trap/24h (± SE)	*Cu. longiareolata* male /trap/24h (± SE)	*Cu. annulata* male /trap/24h (± SE)

Urban parks	6.46 (± 2.80)	3.59 (± 2.89)	3.83 (± 1.97)	1.83 (± 1.67)	1.48 (± 0.79)	0.49 (± 0.38)	0.02 (± 0.02)	0.02 (± 0.02)	0.01 (± 0.01)
Residential areas	3.97 (± 1.64)	1.58 (± 1.14)	3.31 (± 1.65)	0.93 (± 0.83)	0.30 (± 0.16)	0.07 (± 0.05)	0.01 (± 0.01)	0.01 (± 0.01)	0
Impervious built areas	2.91 (± 1.37)	1.19 (± 0.87)	1.99 (± 1.08)	0.72 (± 0.69)	0.26 (± 0.18)	0.16 (± 0.12)	0.01 (± 0.01)	0.01 (± 0.01)	0

SE: Standard error

Bivariate analysis

Vegetation and other land cover variables

Fig 2 shows the vegetation and other land cover variables correlated with the probability of presence or abundance of female *Ae. albopictus*. Two variables related to low vegetation were significantly and positively associated with the probability of presence within a 20 m radius buffer around the traps: the total length (in m) of low vegetation edges (OR =1.007, R^2 =0.042, p =0.042, CI 95% [1.001; 1.014]) and the average patch size (in m^2) of low vegetation (OR =1.01, R^2 =0.07, p =0.006, CI 95% [1.003; 1.017]). The percentage of area occupied by buildings within a 50 m radius buffer around the traps was negatively correlated with the probability of presence (OR =0.959, R^2 =0.047, p =0.048, CI 95% [0.920; 0.999]). Within a 20 m radius buffer around the trap, the total length edge of roads and the average size of a patch of roads were negatively correlated with the probability of presence (Fig 2).

Regarding abundance, positive associations were observed with all vegetation-related variables except for the average patch size of low vegetation within a 50 m radius buffer that showed a negative and significant association (RR =0.996, R^2 =0.098, p =0.0001, CI 95% [0.994;

359 0.998]). The most remarkable positive association was for the total edges length of low
360 vegetation within a 100 m buffer (RR =1.0008, R^2 =0.190, p =0.007, CI 95% [1.0002; 1.0014]).
361 Variables representing the building land cover category consistently showed negative
362 relationships with female *Ae. albopictus* abundance, especially for the percentage area
363 variable (across all buffer radii) and for all variables within the 100m buffer radius. RR for the
364 percentage of buiding areas in the 100m buffer was 0.945 (R^2 =0.240, p =0.0007, CI 95%
365 [0.914; 0.976]) (Fig 2).
366

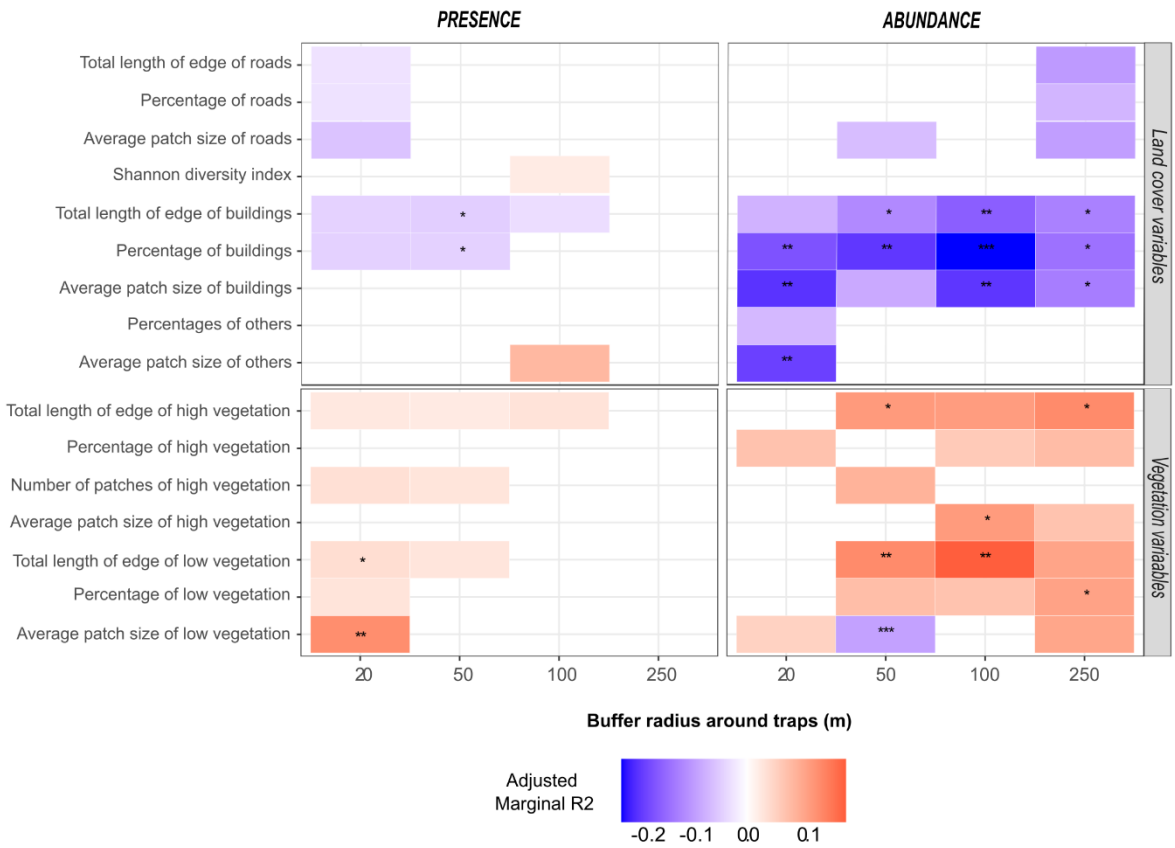

367

368 **Fig 2: Bivariate relationships between *Ae. albopictus* and land cover variables for varied**
369 **buffer sizes**. Relationships are analysed based on *Ae. albopictus* presence or abundance and
370 land cover variables for different buffer sizes around traps. The adjusted marginal R^2 reflects
371 the variance explained by the explanatory variable, adjusted for correlation direction. Boxes

are colored if the p-value was < 0.2 (No asterisk: p-value ∈ [0.05; 0.2], *: p-value ∈ [0.01, 0.05], **: p-value ∈ [0.001; 0.01]; ***: p-value ∈ [0; 0.001]). Box color depend on the direction of the relationship (blue : negative, red : positive). Color intensity vary according to the marginal R^2 value.

Microclimatic, meteorological, and air quality variables

Fig 3 shows the relationship between presence or abundance and microclimatic or meteorological variables recorded from 48h before the start of sampling and during sampling. Local relative humidity (RH) variable showed positive associations with presence when recorded before sampling (with the strongest association for maximum hourly relative humidity 24-48h before sampling; OR = 1.194, R^2 =0.201, p = 0.002, CI 95% [1.070; 1.332]) and negative association when recorded during sampling (with the strongest association for minimum RH; OR =0.924, R^2 =0.134, p = 0.001, CI 95% [0.880;0.969]). Significant associations of RH data with abundance were negative whatever the period considered.

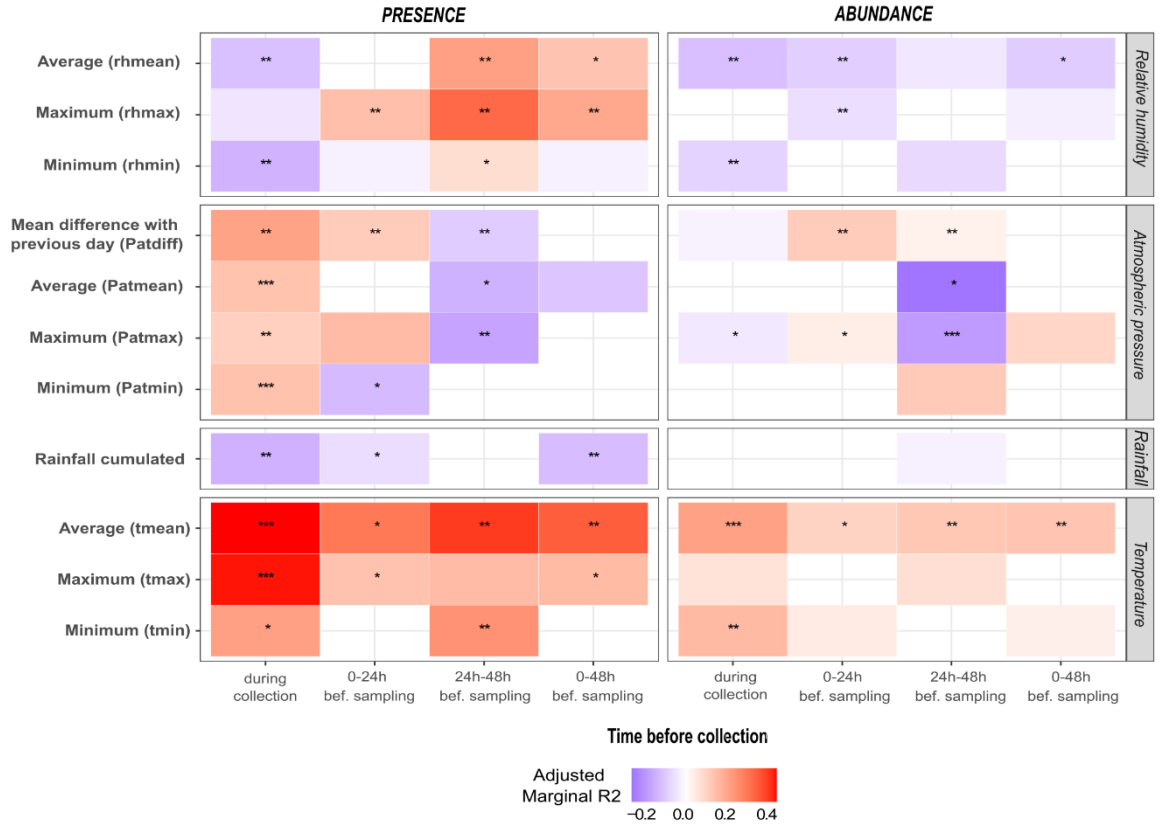

Fig 3: Bivariate relationships between *Ae. albopictus* and microclimatic and meteorological variables 48h before and during sampling. Relationships are analysed base on *Ae. albopictus* presence or abundance and variables recorded 48h before the start and during sampling sessions. Microclimatic variables include minimum hourly relative humidity (rhmin), maximum hourly relative humidity (rhmax), mean hourly relative humidity (rhmean), minimum hourly temperature (tmin), maximum hourly temperature (tmax) and mean hourly temperature (tmean). Meteorological variables include daily cumulated rainfall, minimum atmospheric pressure (Patmin), maximum atmospheric pressure (Patmax), mean atmospheric pressure (Patmean) and the difference of mean atmospheric pressure between two consecutive days (Patdiff). The adjusted marginal R^2 reflects the variance explained by the explanatory variable, adjusted for correlation direction. Boxes are colored if the p-value is < 0.2 (No asterisk: p-value ∈ [0.05; 0.2], *: p-value ∈ [0.01, 0.05], **: p-value ∈ [0.001; 0.01]; ***: p-value ∈ [0; 0.001]).

Box color depend on the direction of the relationship (blue : negative, red : positive). Color intensity vary according to the marginal R^2 value. bef=before

Local temperatures during and before sampling consitently showed positive correlations with presence, particularly for mean and maximum hourly temperatures recorded during sampling (tmean: OR =1.592, R^2 =0.408, p =0.0002, CI 95% [1.251; 2.026]; tmax: OR =1.497, R^2 =0.402, p =0.0001, CI 95% [1.226; 1.828]). Abundance was also positively associated with tmean (RR =1.143, R^2 =0.197, p =0.0002, CI 95% [1.064; 1.228]) and tmax (RR =1.057, R^2 =0.061, p =0.07, CI 95% [0.996; 1.122]) during sampling, but with lower R^2.

Daily total precipitation was negatively associated with presence during sampling (OR =0.863, R^2 =0.137, p =0.003, CI 95% [0.783; 0.951]). *Ae. albopictus* presence was positively associated with all variables describing atmospheric pressure recorded during the sampling hours but negatively with lagged data. The strongest effect size was for the difference in mean daily atmospheric pressure (Patdiff) between the sampling day and the previous day (OR = 1.008, R^2 = 0.194, p = 0.008, CI 95% [1.002; 1.014]). Average (patmean) and maximum (patmax) atmospheric pressure during the 24-48h period preceding sampling showed negative associtaion with abundance (RR =0.997, R^2 =0.243, p =0.018, CI 95% [0.994; 0.999] and RR =0.998, R^2 =0.177, p =0.0001, CI 95% [0.996; 0.999], respectively).

Local temperatures during and before sampling consitently showed positive correlations with female presence, particularly for mean and maximum hourly temperatures recorded during sampling (tmean: OR =1.662, R^2 =0.439, p =0.0001, CI 95% [1.298; 2.129]; tmax: OR =1.553, R^2 =0.424, p =0.0001, CI 95% [1.262; 1.991]). Abundance was also positively associated with

tmean (RR =1.134, R^2 =0.197, p =0.0001, CI 95% [1.055; 1.218]) and tmax (RR =1.052, R^2 =0.050, p =0.098, CI 95% [0.991; 1.117]) during sampling, but with lower R^2.

Daily total precipitation was negatively associated with presence during sampling (OR =0.859, R^2 =0.133, p =0.003, CI 95% [0.777; 0.949]). *Ae. albopictus* presence was positively associated with all variables describing atmospheric pressure recorded during the sampling hours but negatively with lagged data. The strongest effect size was for the difference in mean daily atmospheric pressure (Patdiff) between the sampling day and the previous day (OR = 1.008, R^2 = 0.217, p = 0.003, CI 95% [1.003; 1.015]). Average (patmean) and maximum (patmax) atmospheric pressure during the 24-48h period preceding sampling showed negative associtaion with abundance (RR =0.997, R^2 =0.217, p =0.049, CI 95% [0.994; 0.999] and RR =0.998, R^2 =0.183, p =0.0003, CI 95% [0.996; 0.999], respectively).

Fig 4 shows the effect size and significance ($p < 0.2$) of weeks-lagged meteorological variables on the presence and abundance of female *Ae. albopictus*. The relationship between weekly cumulated rainfall (CUMRF) and both the probability of presence and abundance was positive, with a statistically significant association for abundance and the highest effect size observed the 6th week before sampling (for presence: OR = 1.430, R^2 = 0.334, p = 0.168, CI 95% [0.860; 2.375]; for abundance: RR = 1.075, R^2 = 0.127, p = 0.04, CI 95% [1.003; 1.152]). The probability of presence was positively and significantly associated with minimum (TMIN), average (TMEAN), and maximum (TMAX) temperatures. The highest effect size was observed for TMIN one week before sampling (OR =1.620, R^2 =0.372, p =0.001, CI 95% [1.209; 2.172]. For abundance, relationships with TMIN, TMEAN, and TMAX were also positive and significant for time interval 0 to 2 weeks before sampling, with the highest effect size observed for TMAX (RR = 1.161, R^2 =0.192, p = 0.0006, CI 95% [1.067; 1.267]). Both responses were positively and

448 significantly correlated with the weekly growing degree days (GDD). The highest effect on
449 presence and abundance was observed for GDD during the week preceding sampling (OR =
450 1.085, R^2 = 0.357, p = 0.002, CI 95% [1.031; 1.141]) and for time interval 0 to 2 weeks before
451 sampling (RR = 1.011, R^2 = 0.189, p = 0.0009, CI 95% [1.004; 1.017]), respectively. Both
452 responses were negatively and significantly correlated with relative humidity (RH), with the
453 highest effect observed for RH recorded 6 weeks before sampling (OR = 0.792, R^2 = 0.472, p
454 = 0.006, CI 95% [0.670; 0.937] for presence; RR = 0.948, R^2 = 0.183, p = 0.007, CI 95% [0.912;
455 0.986] for abundance). The relationship between wind speed (WS) and abundance was
456 negative, with the highest effect observed for time interval 0 to 5 weeks before collection (RR
457 =0.343, R^2 = 0.086, p =0.157, CI 95% [0.078; 1 .510]).

458

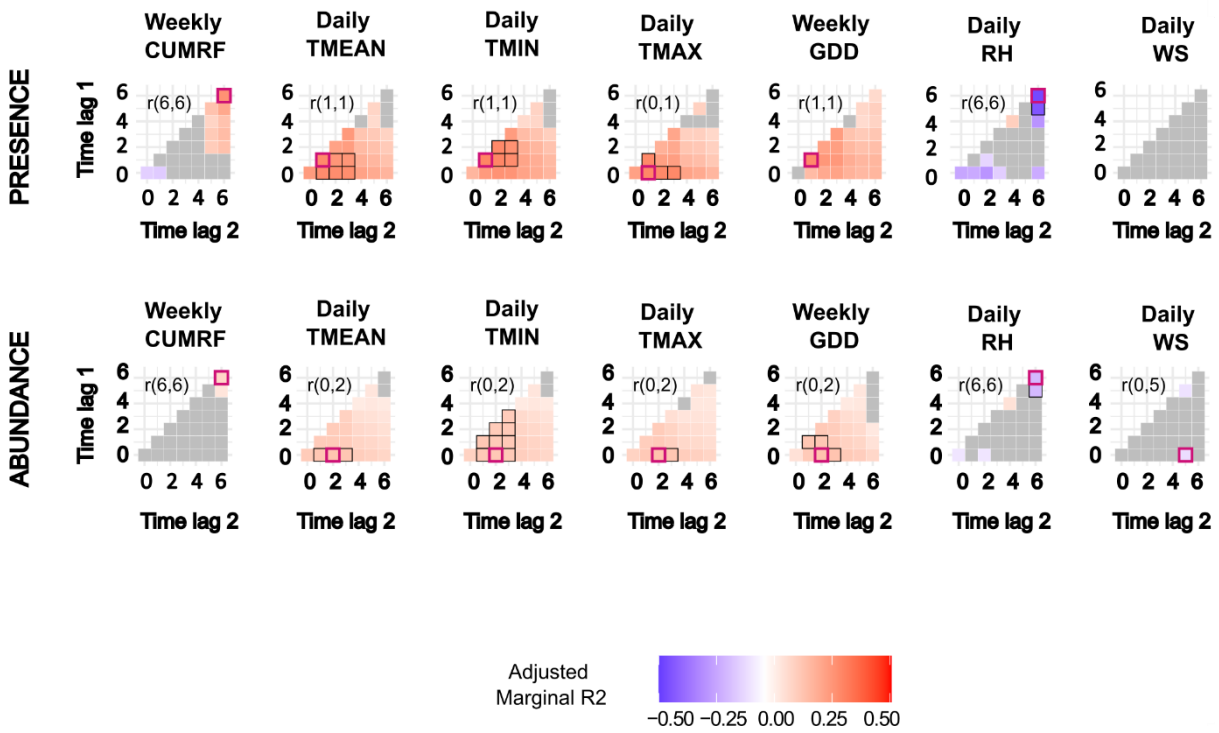

459

460

461 **Fig 4: Cross correlation maps showing the lagged effect of meteorological variables on *Ae.***
462 ***albopictus* presence or abundance**. Lagged meteorological variables include weekly

463 cumulated daily rainfall (CUMRF), mean daily temperature (TMEAN), daily minimal
464 temperature (TMIN), daily maximal temperature (TMAX), the weekly Growing Degree Days
465 (GDD), mean daily relative humidity (RH), and mean daily wind speed (WS). Time lags are
466 expressed in weeks prior to sampling. The adjusted marginal R^2 reflects the variance explained
467 by the explanatory variable, adjusted for correlation direction. Red-bordered squares highlight
468 the time lag with the highest marginal R^2, with the interval indicated in the top left corner.
469 Black-bordered squares denote marginal R^2 values close to the highest (within 10%). Gray
470 squares represent correlations with p-values > 0.2.
471
472 Daily nitrogen dioxide (NO2) concentrations were positively associated with the probability of
473 presence of female *Ae. albopictus*, with the highest effect size observed for the sampling week
474 (OR = 1.109, R^2 = 0.126, p = 0.163, CI 95% [0.959; 1.282]; S5 Fig). Particulate matter
475 concentrations (PM2.5 and PM10) were also positively correlated with the probability of
476 presence and with the abundance. However, PM2.5 and PM10 concentrations were strongly
477 correlated with all time-lagged temperature metrics (Pearson coefficient > 0.8). Tropospheric
478 ozone (O3) concentration (three weeks before sampling) was negatively correlated with the
479 probability of presence and positively (one week before sampling) with abundance. Daily O3
480 concentrations were also highly correlated with weekly cumulated rainfall, wind speed, and
481 daily relative humidity (Pearson coefficient > 0.8).
482

483 **Socio-demographic variables**

484 Human population density in a 250 m radius buffer around traps was positively correlated
485 with the *Ae. albopictus* probability of presence (OR=1.0013, R2=0.056, p=0.029, CI 95%
486 [1.0001; 1.0026]; S6 Fig).

Multivariate analysis

After bivariate analyses, multicollinearity assessments, and recursive feature elimination, ten and seven variables, in addition to sampling design variables, were kept for the multivariate random forest models of presence and abundance, respectively (S5 Table shows reason for exclusion). Fig 5 and Fig 6 display the multivariate RF model interpretation plots for presence and abundance, respectively. Fig 5A and Fig 6A illustrate the contribution of each variable in explaining the response variable (VIPs). Fig 5B and Fig 6B depict the relationship between the response variable and the explanatory variables (PDPs). Models of presence and abundance did not show any residual spatial autocorrelation.

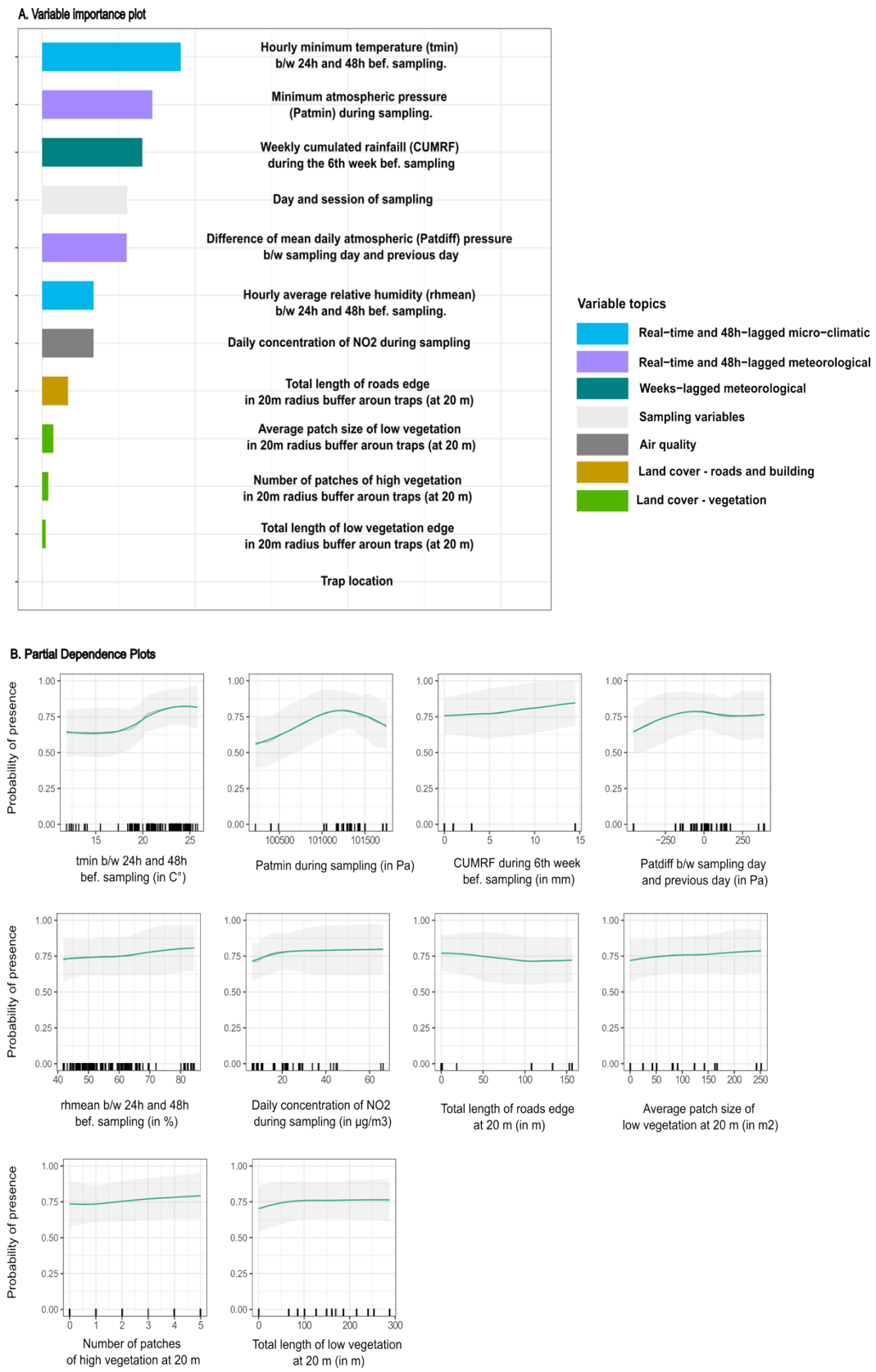
A. Variable importance plot
Hourly minimum temperature (tmin) b/w 24h and 48h bef. sampling.
Minimum atmospheric pressure (Patmin) during sampling.
Weekly cumulated rainfaill (CUMRF) during the 6th week bef. sampling
Day and session of sampling
Difference of mean daily atmospheric (Patdiff) pressure b/w sampling day and previous day
Hourly average relative humidity (rhmean) b/w 24h and 48h bef. sampling.
Daily concentration of NO2 during sampling
Total length of roads edge in 20m radius buffer aroun traps (at 20 m)
Average patch size of low vegetation in 20m radius buffer aroun traps (at 20 m)
Number of patches of high vegetation in 20m radius buffer aroun traps (at 20 m)
Total length of low vegetation edge in 20m radius buffer aroun traps (at 20 m)
Trap location
Variable topics
Real−time and 48h−lagged micro−climatic
Real−time and 48h−lagged meteorological
Weeks−lagged meteorological
Sampling variables
Air quality
Land cover - roads and building
Land cover - vegetation
B. Partial Dependence Plots
Probability of presence
tmin b/w 24h and 48h bef. sampling (in C°)
Patmin during sampling (in Pa)
CUMRF during 6th week bef. sampling (in mm)
Patdiff b/w sampling day and previous day (in Pa)
rhmean b/w 24h and 48h bef. sampling (in %)
Daily concentration of NO2 during sampling (in µg/m3)
Total length of roads edge at 20 m (in m)
Average patch size of low vegetation at 20 m (in m2)
Number of patches of high vegetation at 20 m
Total length of low vegetation at 20 m (in m)

Fig 5: **Interpretation plots for the multivariate random forest model of *Ae. albopictus* presence**. The left plot (Fig 5A) is the variable importance plot (VIP). Rights plots (Fig 5B) are smoothed partial dependence plots (PDPs) with Confidence Intervals for each selected variable in the models. The y-axis in PDPs represents the probability of catching at least one mosquito. The range of values in the x-axis represents the range of values available in the data for the considered variable. The rugs above the x-axis represent the actual values available in the data for the variable. The black line represents the unsmoothed PDP, while the green line shows the smoothed version. The shaded gray area corresponds to the 95% confidence intervals, calculated using the standard deviation and adjusted for local data density. b/w: between. bef.: before. tmin: minimum hourly temperature. rhmean: hourly average relative humidity. Patmin: minimum daily atmospheric pressure. Patdiff: difference of mean daily atmospheric pressure. CUMRF: Cumulated Rainfall.

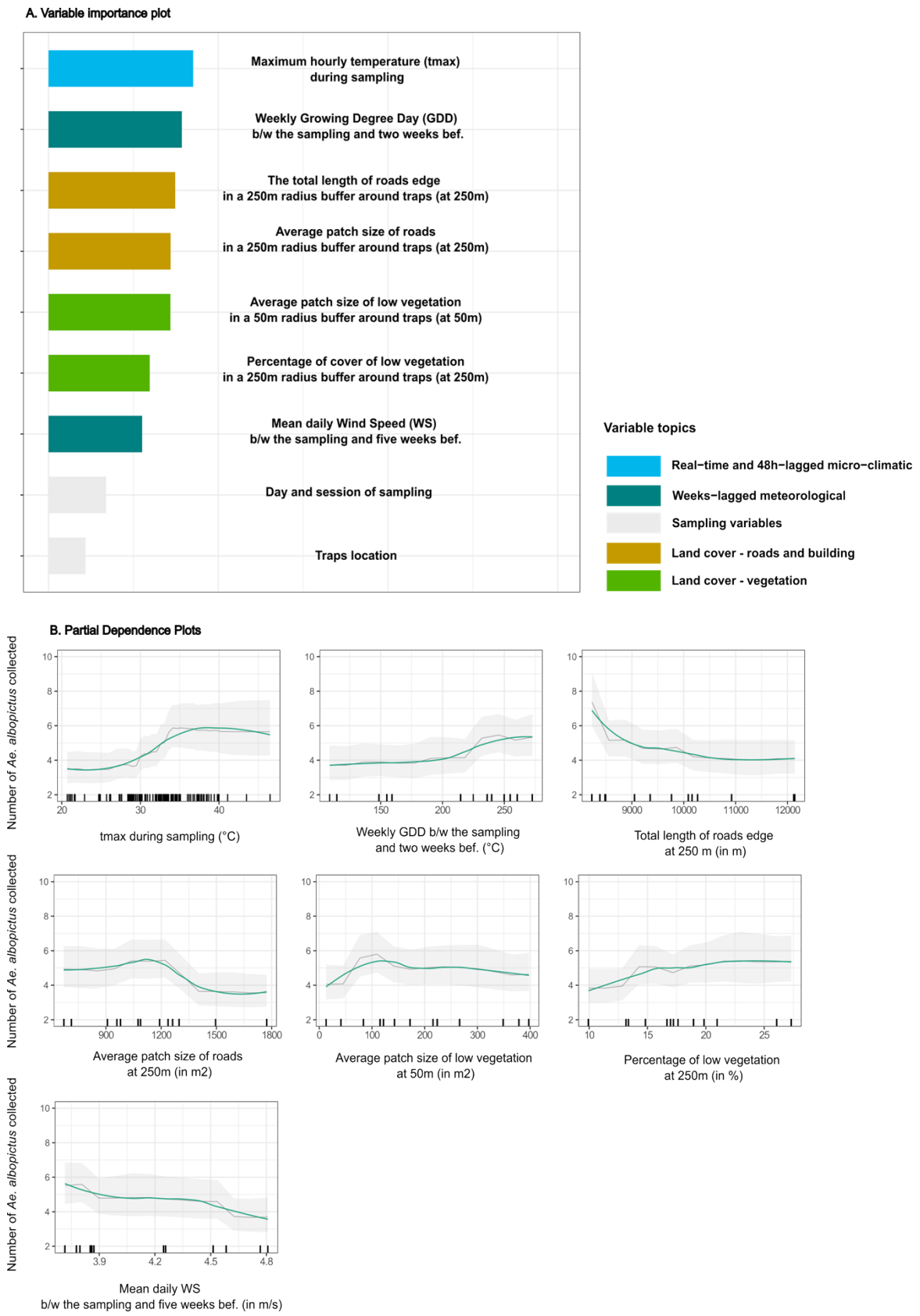

Fig 6: Interpretation plots for the multivariate random forest model of *Ae. albopictus* abundance. The left plot (Fig 6A) is the variable importance plot (VIP). Rights plots (Fig 6B) are

515 smoothed partial dependence plots (PDPs) with Confidence Intervals for each selected
516 variable in the models. The y-axis in PDPs represents the number of *Ae. albopictus* females
517 caught/trap/24h. The range of values in the x-axis represents the range of values available in
518 the data for the considered variable. The rugs above the x-axis represent the actual values
519 available in the data for the variable. The black line represents the unsmoothed PDP, while
520 the green line shows the smoothed version. The shaded gray area corresponds to the 95%
521 confidence intervals, calculated using the standard deviation and adjusted for local data
522 density. b/w: between. bef.: before. tmax: maximum hourly temperature. GDD: Growing
523 Degree Day. WS: Wind Speed
524

525 **Presence model**

526 The most contributing variables to presence probability were a combination of real-time and
527 time-lagged microclimatic and meteorological variables (Fig 5A), with only a minimal
528 contribution of vegetation variables. The first contributing variable was the local minimum
529 hourly temperature recorded 24–48 hours before sampling. The probability of presence
530 showed a slight increase between 11.9°C and 16°C, rose sharply from 16°C to 25°C, and
531 plateaued beyond 25°C (Fig 5B). Minimum atmospheric pressure during sampling was the
532 second most influential variable, with an unimodal relationship: presence probability
533 increased up to 1012.91 HPa before declining. Cumulated rainfall 6 weeks before sampling
534 emerged as the third key variable, displaying a linear positive association with presence
535 probability, from 0 mm to 15 mm. The fourth major factor was the mean daily atmospheric
536 pressure difference between the sampling and previous day. Presence probabilities decreased
537 for descreasing pressures and was stable for stable or increasing pressures. Secondary
538 contributors included mean local hourly relative humidity 24–48 hours before sampling, daily

539 NO_2 concentrations, and vegetation metrics within a 20 m buffer around traps (average patch
540 size of low vegetation, number of high vegetation patches, and total length of low vegetation
541 edges). These variables slightly increased presence probability, whereas the total length of
542 edges of roads in a 20 m radius buffer weakly reduced it. The model demonstrated strong
543 predictive accuracy (AUC = 0.89; S7A Fig). Cross-validation with the leave-area-out method
544 produced consistent predictions, except in the impervious Diderot School area (IMP-DID). In
545 contrast, leave-sampling-session-out cross-validation exhibited greater variability between
546 sampling areas (S7B Fig).
547

548 **Abundance model**

549 The most contributing variables to *Ae. albopictus* abundance comprised a combination of
550 microclimatic, weeks-lagged meteorological, vegetation and other land cover variables. The
551 first contributing variable was the local maximum hourly temperature during sampling (Fig
552 6A). A strong positive correlation with abundance was observed between 24°C and 38.7°C,
553 followed by a negative correlation beyond 40.6°C (Fig 6B). The second most important variable
554 was the weekly GDD between the sampling day and two weeks prior, which exhibited a linear
555 positive correlation with abundance. The third key variable was the total length of road edges
556 within a 250 m buffer around traps, with a strong negative correlation between 8230 m and
557 11 000 m. The fourth key variable was the average size of road patches within a 250 m buffer.
558 It had no effect on abundance up to 1110 m² but exhibited a negatively correlation with
559 abundance at sizes greater than 1630 m². The next variable was the average size of low-
560 vegetation patches within a 50 m radius buffer around traps**.** Abundance increased markedly
561 for areas between 0 and 120 m², plateaued up to 237 m², and subsequently decreased slightly.
562 The percentage of low vegetation in a 250 m radius buffer around traps was positively

563 correlated with abundance between 10% and 23%, beyond which it had no observable effect.
564 Finally, average wind speed between day of sampling and five weeks before had no effect on
565 abundance between 3.7 m/s and 4.3 m/s, but showed a negative correlation beyond this
566 range. The abundance model demonstrated good overall accuracy, except for high abundance
567 cases (>11 mosquitoes, Mean Absolute Error (MAE)=7.86, S8A Fig). Spatial cross-validation
568 retained overall abundance trends, except in RES-LEM and PRK-AIG, and showed an
569 underestimation of high abundance and an overestimation of low abundance. Temporal cross-
570 validation, using leave-sampling-session-out, did not preserve abundance trends but captured
571 relative differences in *Ae. albopictus* abundance between areas (S8B Fig).
572

573 # Discussion

574

575 This study examined, for the first time in France, the impact of urban vegetation on the
576 presence and abundance of *Ae. albopictus*, showing a minimal influence on the presence and
577 a moderate positive association with the abundance. The analytical methodology employed
578 in this study provides a nuanced evaluation of how different environmental factors contribute
579 to mosquito presence and abundance. It highlights the existence of non-linear relationships,
580 offering valuable insights for identifying effective vector control measures.
581

582 ## Influence of urban vegetation and other land cover variables

583

584 This study highlights that urban vegetation within a 20 m buffer radius around traps had a
585 minimal weakly positive influence on the probability of the presence of *Ae. albopictus*.

Regarding the abundance, urban vegetation demonstrated a moderate positive effect. This positive effect of urban vegetation on the abundance of *Ae. albopictus* has also been observed in other countries, including Italy [26], Brazil [88], Singapore [89], and China [33]. In our study, the first vegetation metric influencing abundance was the average size of low-vegetation patches within a 50 m buffer radius. These findings are consistent with those of Cianci *et al* (2015) [26], who reported a positive relationship between vegetation cover within a 50 m radius buffer around traps and *Ae. albopictus* eggs abundance in Italy. Manica *et al* (2016) observed that, in Roma (Italy), vegetation cover within a 20 m radius around traps positively influenced *Ae. albopictus* female abundance [27]. They hypothesised that the tiger mosquito prefers "small green islands". Our findings refine this hypothesis by demonstrating that *Ae. albopictus* abundance significantly increases with the average size of low-vegetation patches, particularly within the 10 to 120 m² range. Beyond 120 m², the effect stabilises. This nuance provides additional detail to the assumption proposed by Manica *et al*. This hypothesis, along with the identified size range, requires further research to confirm its generalisability across different urban contexts and mosquito populations.

The percentage of low vegetation cover within a 250 m radius around traps moderately increased abundance. These results are consistent with the study of Sun *et al* (2021), which demonstrated that, in Singapore, *Ae. albopictus* abundance increased with managed vegetation within a 300 m radius buffer around traps [89]. However, Manica *et al* (2016) found a negative relationship between vegetation cover within a 300 m radius buffer and mosquito abundance [27]. These differences can be attributed to variations in city architecture and study design. In our study, the percentage of low vegetation cover ranged from 10% to 23.5%, whereas in Manica *et al*, it ranged from 30% to 55%. With different ranges of vegetation cover,

differing study designs, and contrasting urban environments, direct comparisons are challenging.

The other two land cover variables, the third and fourth contributors to abundance, are road metrics within a 250 m radius buffer around traps. The first was the total length of road edges, which was negatively correlated with abundance. These findings aligned with the study by Wang *et al* (2023) in Shanghai (China) which reported a negative correlation between road length and *Ae. albopictus* eggs density [33]. This supports our initial assumption that roads act as barriers to mosquito movement. This hypothesis was also consistent with Regilme *et al* (2021), who observed genetic differentiation in *Ae. aegypti* populations located north and south of a major road in Shanghai [42]. The second road-related variable was the average size of road patches. Roads may represent unfavorable habitats for host-seeking *Ae. albopictus* which could explain their limited abundance in areas dominated by large roads.

Influence of microclimatic and meteorological variables

The relationship between atmospheric pressure and the presence of *Ae. albopictus* in the field has, to our knowledge, been investigated for the first time in this study. The minimum atmospheric pressure during the 24-hour sampling period and the difference in daily mean atmospheric pressure between the sampling day and the previous day were the second and fourth main variables contributing to presence. Haufe (1954) demonstrated that atmospheric pressure affects the flight activity of *Ae. aegyp*ti, especially the change in atmospheric pressure after six hours of acclimatisation [53]. A study by Knop *et al* (2023) in Switzerland showed that the traffic rate of high-flying insects (number of insects per hour) had a positive correlation with air pressure [90]. Our results suggest an effect of the atmospheric pressure

633 metrics on the activity and behaviour of the tiger mosquito. Further studies under controlled
634 laboratory and field conditions are needed to investigate these findings in more detail.
635 Local hourly temperatures were the first variables to contribute to both presence and
636 abundance. Evans *et al* (2019) found an exponential relationship between the minimum
637 temperature during the 7 days preceding sampling and the abundance of females, as well as
638 an unimodal relationship between the maximum temperature and the abundance of females,
639 with an optimal daily maximum temperature around 35°C [32]. Our results suggest that
640 increasing daily maximum temperature increases the activity of *Ae. albopictus* up to 38°C.
641 The third variable influencing the presence of *Ae. albopictus* was the weekly cumulated rainfall
642 recorded six weeks before sampling. While other studies have identified a positive
643 relationship between *Ae. albopictus* dynamics and rainfall accumulated over several weeks
644 before sampling, none have specifically examined a six-week delay. Roiz *et al* (2015) observed
645 in Montpellier that strong rainfall, particularly that accumulated each week over the four
646 weeks before sampling, positively influenced abundance [31]. Similarly, Manica *et al* (2016)
647 reported a positive relationship between the cumulated rainfall one month before sampling
648 and mosquito abundance [27]. The positive effect of rainfall in our study may be explained by
649 the filling of larval habitats, benefiting previous mosquito generations that influenced the
650 sampled population. This hypothesis requires confirmation through additional temporal
651 replicates to validate the observed trend.
652 The second most influential variable of abundance was the weekly GDD during the two weeks
653 preceding sampling. Based on minimum, maximum, and average temperatures, the GDD is
654 widely used as a key predictor for many insect species [91]. For *Ae. albopictus*, the GDD is
655 calculated using a baseline temperature of 11°C, promoting mosquito development when
656 temperatures exceed this value [50]. This baseline corresponds to the average annual

temperature required for the spread of *Ae. albopictus* [92]. Jourdain *et al* (2020) identified the GDD as the primary predictor of population dynamics for this species [93].

The last variable influencing abundance is the mean daily wind speed during the five weeks preceding sampling. Le Goff *et al* (2024) observed a similar negative relationship between monthly average daily wind speed and *Ae. albopictus* eggs abundance on the Réunion Island [94]. Adeleke *et al* (2022) reported that in regions where the tiger mosquito is present, wind speeds exceeding 4 $m \cdot s^{-1}$ reduce the likelihood of occurrence [95]. The threshold identified in our study (4.3 $m \cdot s^{-1}$) can be considered comparable to the findings of Adeleke *et al*, although direct comparisons between the studies are challenging due to differences in spatial and temporal scales.

Limitations, perspectives and conclusion

In order to increase the resilience of Urban Green Infrastructures (UGIs) [96] and to adapt the UGIs management to promote biodiversity [97], since 2017, studies have highlighted the need to consider UGIs as socio-ecological ecosystems. This reflects the complexity of urban greening, which must account for land cover, socio-demographic variables, and urban architecture, as demonstrated in the systematic review by Menconi *et al* (2021) [98]. The challenge of studying the relationship between urban greening and the risk of vector-borne diseases is one of the key conclusions of the scoping review by Mercat *et al* (2025) [24]. The difficulty stems from the need to integrate multiple variables essential to the analysis of this socio-ecosystem, the time required to observe its effects [28], and the challenge of assessing vector-borne disease risk using standardised protocols.

680 Due to limited financial and human resources, this study was limited to specific sampling areas
681 within vegetated environments representative of the city's UGS and non-vegetated
682 environments. A randomised sampling approach would have better captured the diversity of
683 land cover categories. In order to reduce interference between traps less than 50 m apart,
684 averages of meteorological, microclimatic, landscape and ethological variables were
685 calculated. The predicted abundance of *Ae. albopictus* in the RES-SOUL residential area was
686 therefore certainly underestimated. While the abundance model effectively captures
687 temporal variation, it does not account well for spatial variation. This suggests that key factors
688 such as environmental carrying capacity, defined as the 'equilibrium density of larvae in a
689 system' [99], and the availability of resting sites may have been overlooked (35). This is also
690 related to the complexity of describing urban vegetation using remote sensing [24]. In our
691 study, we employed a fine-scale characterisation of urban vegetation generated through deep
692 learning and photo interpretation, alongside a surface modelling metric derived from lidar
693 data. However, this approach does not capture the diversity of plant species or genera, which
694 can vary markedly between the Botanical Garden, the Park of Aiguelongue, and residential
695 areas.
696 The objectives of this study were to explore the relationships between urban vegetation and
697 other environmental factors with the presence and abundance of *Ae. albopictus*, to generate
698 hypotheses using an exploratory approach. The realisation of predictive model is another
699 objective, which requires a better understanding of the ecological and biological mechanisms
700 [100]. The results of the study are based on only one sampling year. To draw more robust
701 conclusions, additional years of sampling would be needed to assess inter-annual variation. In
702 addition, this study has focused solely on one aspect of the vector risk, the presence and
703 abundance of the vector, without considering its capacity to transmit pathogens, or human

exposure and vulnerability. The vector's capacity depends on the abundance of females, the daily survival rate, and the extrinsic incubation period of pathogens [101]. It would be relevant to investigate the effect of urban vegetation on these elements. Together with these investigations, a socio-ecological approach is essential to gain a comprehensive understanding of vector-borne disease risks in urban green spaces. Developing social surveys to assess citizens' perceptions, alongside employing co-construction methods [102] with policymakers, urban designers, and ecologists, could help formulate effective recommendations to mitigate this risk. One example could be the development of green wind corridors, as implemented in Stuttgart [103] and Lisbon [104], which can reduce urban heat islands and increase wind speed, limiting mosquito abundance.

Urban greening appears to be a promising solution to address the environmental and health challenges associated with increasing urbanisation. It offers numerous health and environmental benefits, but can also contribute to an increased risk of vector-borne diseases. This study, the first in France to investigate the effect of urban vegetation on *Ae. albopictus*, provides a nuanced assessment of how urban vegetation influences both the presence and abundance of mosquitoes. Our results indicate that urban vegetation moderately increases abundance, but has no effect on presence. Urban greening is a dynamic and complex phenomenon that requires a social-ecological approach in order to be studied. Further research is needed to better elucidate the role of urban vegetation in the ecology of the tiger mosquito and its influence on different aspects of risk.

Acknowledgements

We would also like to thank Gilbert Le Goff, Nil Rahola, Christophe Pauoy for the help to the design sampling and Mathilde Mercat, Coralie Grail and all the other field and laboratory staff for their strong commitment to the V2MOC project. We would like to thank the managers and staff of the Botanical Garden who facilitated our access, the managers of the green spaces of the city of Montpellier for access to the Parc de l'Aiguelongue, as well as the managers of the Insituts Diderot, Bouisson Bertrand, the Hotel Acapulco and the Saint Charles site of the University of Montpellier III, as well as the individuals who gave us access to their gardens. We thank all the persons who worked on the open access databases used in this work.

References

1. Manzoor Hussain, Imitiaz I. Urbanization concepts, dimension and factors. Int J Recent Sci Res. 2018;

2. Breuste J, Niemelä J, Snep RPH. Applying landscape ecological principles in urban environments. Landsc Ecol. 2008 Dec;23(10):1139–42.

3. Zhang Z, Zhao M, Zhang Y, Feng Y. How does urbanization affect public health? New evidence from 175 countries worldwide. Front Public Health. 2023 Jan 6;10:1096964.

4. Xu X, Xie Y, Qi K, Luo Z, Wang X. Detecting the response of bird communities and biodiversity to habitat loss and fragmentation due to urbanization. Sci Total Environ. 2018 May;624:1561–76.

5. Qi F, Abu-Rumman A, Al Shraah A, Muda I, Huerta-Soto R, Hai Yen TT, *et al*. Moving a step closer towards environmental sustainability in Asian countries: focusing on real income, urbanization, transport infrastructure, and research and development. Econ Res-Ekon Istraživanja. 2023 Jul 10;36(2):2111317.

750 6. Moore M, Gould P, Keary BS. Global urbanization and impact on health. Int J Hyg Environ Health.
751 2003;206(4–5):269–78.

752 7. Ventriglio A, Torales J, Castaldelli-Maia JM, De Berardis D, Bhugra D. Urbanization and emerging
753 mental health issues. CNS Spectr. 2021 Feb;26(1):43–50.

754 8. Almusaed A. The Urban Heat Island phenomenon upon urban components. In: biophilic and
755 bioclimatic architecture [Internet]. London: Springer London; 2011 [cited 2024 Sep 18]. p. 139–
756 50. Available from: http://link.springer.com/10.1007/978-1-84996-534-7_10

757 9. Heaviside C, Macintyre H, Vardoulakis S. The Urban Heat Island: implications for health in a
758 changing environment. Curr Environ Health Rep. 2017 Sep;4(3):296–305.

759 10. United Nations (UN). Goal 11: Make cities and human settlements inclusive, safe, resilient and
760 sustainable. New York: UN. [Internet]. [cited 2024 Nov 19]. Available from:
761 https://sdgs.un.org/goals/goal11

762 11. Unit B. Convention on Biological Diversity [Internet]. Secretariat of the convention on biological
763 diversity; 2022 [cited 2024 Oct 2]. Available from: https://www.cbd.int/gbf/targets/12

764 12. The European Green Deal: A growth strategy that protects the climate [Internet]. 2022 [cited
765 2024 Oct 2]. Available from: https://ec.europa.eu/stories/european-green-deal

766 13. Chang J, Qu Z, Xu R, Pan K, Xu B, Min Y, *et al.* Assessing the ecosystem services provided by
767 urban green spaces along urban center-edge gradients. Sci Rep. 2017 Sep 11;7(1):11226.

768 14. Liu HL, Shen YS. The impact of green space changes on air pollution and microclimates: a case
769 study of the Taipei metropolitan area. Sustainability. 2014 Dec 3;6(12):8827–55.

770 15. Gunawardena KR, Wells MJ, Kershaw T. Utilising green and bluespace to mitigate urban heat
771 island intensity. Sci Total Environ. 2017 Apr;584–585:1040–55.

16. Callaghan A, McCombe G, Harrold A, McMeel C, Mills G, Moore-Cherry N, *et al*. The impact of green spaces on mental health in urban settings: a scoping review. J Ment Health. 2021 Mar 4;30(2):179–93.

17. Zhang Y, Meng W, Yun H, Xu W, Hu B, He M, *et al*. Is urban green space a carbon sink or source? - A case study of China based on LCA method. Environ Impact Assess Rev. 2022 May;94:106766.

18. Threlfall CG, Mata L, Mackie JA, Hahs AK, Stork NE, Williams NSG, *et al*. Increasing biodiversity in urban green spaces through simple vegetation interventions. Beggs J, editor. J Appl Ecol. 2017 Dec;54(6):1874–83.

19. Cariñanos P, Casares-Porcel M. Urban green zones and related pollen allergy: A review. Some guidelines for designing spaces with low allergy impact. Landsc Urban Plan. 2011 Jun;101(3):205–14.

20. Ciceoi R, Gutue C, Gutue M, Roşca I. Current status of pests associated with urban vegetation in Bucharest area.

21. Lõhmus M, Balbus J. Making green infrastructure healthier infrastructure. Infect Ecol Epidemiol. 2015 Jan;5(1):30082.

22. Fournet F, Simard F, Fontenille D. Green cities and vector-borne diseases: emerging concerns and opportunities. Eurosurveillance [Internet]. 2024 Mar 7 [cited 2024 Aug 19];29(10). Available from: https://www.eurosurveillance.org/content/10.2807/1560-7917.ES.2024.29.10.2300548

23. Heylen D, Lasters R, Adriaensen F, Fonville M, Sprong H, Matthysen E. Ticks and tick-borne diseases in the city: Role of landscape connectivity and green space characteristics in a metropolitan area. Sci Total Environ. 2019 Jun;670:941–9.

24. Mercat M, Bartholomée C, Fournet F, Alcover Amengual M, Bourquia M, Bouhsira E, *et al*. Green cities and the risk for vector-borne disease transmission: a scoping review. 2025. Manuscript under review.

25. Krol L, Langezaal M, Budidarma L, Wassenaar D, Didaskalou EA, Trimbos K, *et al*. Distribution of *Culex pipiens* life stages across urban green and grey spaces in Leiden, The Netherlands. Parasit Vectors. 2024 Jan 29;17(1):37.

26. Cianci D, Hartemink N, Zeimes CB, Vanwambeke SO, Ienco A, Caputo B. High resolution spatial analysis of habitat oreference of *Aedes albopictus* (Diptera: Culicidae) in an urban environment. J Med Entomol. 2015 May 1;52(3):329–35.

27. Manica M, Filipponi F, D'Alessandro A, Screti A, Neteler M, Rosà R, *et al*. Spatial and temporal hot spots of *Aedes albopictus* abundance inside and outside a South European Metropolitan area. McCall PJ, editor. PLoS Negl Trop Dis. 2016 Jun 22;10(6):e0004758.

28. Mata L, Hahs AK, Palma E, Backstrom A, Johnston N, King T, et al. Large positive ecological changes of small urban greening actions. Ecol Solut Evid. 2023 Jul;4(3):e12259.

29. Paupy C, Delatte H, Bagny L, Corbel V, Fontenille D. *Aedes albopictus*, an arbovirus vector: From the darkness to the light. Microbes Infect. 2009 Dec;11(14–15):1177–85.

30. Bonizzoni M, Gasperi G, Chen X, James AA. The invasive mosquito species *Aedes albopictus*: current knowledge and future perspectives. Trends Parasitol. 2013 Sep;29(9):460–8.

31. Roiz D, Boussès P, Simard F, Paupy C, Fontenille D. Autochthonous Chikungunya transmission and extreme climate events in Southern France. Carvalho MS, editor. PLoS Negl Trop Dis. 2015 Jun 16;9(6):e0003854.

32. Evans MV, Hintz CW, Jones L, Shiau J, Solano N, Drake JM, *et al*. Microclimate and larval habitat density predict adult *Aedes albopictus* abundance in urban areas. Am J Trop Med Hyg. 2019 Aug 7;101(2):362–70.

33. Wang F, Zhu Y, Zhang H, Fan J, Leng P, Zhou J, *et al*. Spatial and temporal analyses of the influences of meteorological and environmental factors on *Aedes albopictus* (Diptera: Culicidae) population dynamics during the peak abundance period at a city scale. Acta Trop. 2023 Sep;245:106964.

34. Murdock CC, Evans MV, McClanahan TD, Miazgowicz KL, Tesla B. Fine-scale variation in microclimate across an urban landscape shapes variation in mosquito population dynamics and the potential of *Aedes albopictus* to transmit arboviral disease. Scarpino SV, editor. PLoS Negl Trop Dis. 2017 May 30;11(5):e0005640.

35. Samson DM, Qualls WA, Roque D, Naranjo DP, Alimi T, Arheart KL, *et al*. Resting and energy reserves of *Aedes albopictus* collected in common landscaping vegetation in St. Augustine, Florida. J Am Mosq Control Assoc. 2013 Sep;29(3):231–6.

36. Chabasse D. *Aedes albopictus*, le “moustique tigre”, vecteur de la dengue, du chikungunya et du Zika, s’implante durablement en France métropolitaine. Rev Francoph Lab. 2023 Nov;2023(556):51–9.

37. Climate Data. Climat Montpellier: pluviométrie et température moyenne Montpellier, diagramme ombrothermique pour Montpellier [Internet]. 2020 [cited 2024 Oct 2]. Available from: https://fr.climate-data.org/europe/france/languedoc-roussillon/montpellier-1126/

38. Kermap. Nos villes vertes : la carte de France de la nature en ville [Internet]. 2023 [cited 2024 Oct 2]. Available from: https://www.nosvillesvertes.fr/Accueil

836 39. Russell RC, Webb CE, Williams CR, Ritchie SA. Mark–release–recapture study to measure
837 dispersal of the mosquito *Aedes aegypti* in Cairns, Queensland, Australia. Med Vet Entomol.
838 2005 Dec;19(4):451–7.

839 40. Marini F, Caputo B, Pombi M, Tarsitani G, Della Torre A. Study of *Aedes albopictus* dispersal in
840 Rome, Italy, using sticky traps in mark-release-recapture experiments. Med Vet Entomol. 2010
841 Dec;24(4):361–8.

842 41. Hemme RR, Thomas CL, Chadee DD, Severson DW. Influence of urban landscapes on population
843 dynamics in a short-distance migrant mosquito: evidence for the Dengue vector *Aedes aegypti*.
844 Gubler DJ, editor. PLoS Negl Trop Dis. 2010 Mar 16;4(3):e634.

845 42. Regilme MAF, Carvajal TM, Honnen A, Amalin DM, Watanabe K. The influence of roads on the
846 fine-scale population genetic structure of the dengue vector *Aedes aegypti* (Linnaeus).
847 Bonizzoni M, editor. PLoS Negl Trop Dis. 2021 Feb 26;15(2):e0009139.

848 43. L'Ambert G, Gendrot M, Briolant S, Nguyen A, Pages S, Bosio L, et al. Analysis of trapped
849 mosquito excreta as a noninvasive method to reveal biodiversity and arbovirus circulation. Mol
850 Ecol Resour. 2023 Feb;23(2):410–23.

851 44. Le Goff G, Damiens D, Payet L, Ruttee AH, Jean F, Lebon C, *et al*. Enhancement of the BG-sentinel
852 trap with varying number of mice for field sampling of male and female *Aedes albopictus*
853 mosquitoes. Parasit Vectors. 2016 Dec;9(1):514.

854 45. Gunay F, Picard M, Robert V. MosKeyTool, an interactive identification key for mosquitoes of
855 Euro-Mediterranean. [Internet]. 2017. Available from: www.medilabsecure.com/moskeytool.

856 46. Bartholomée C, Taconet P, Mercat M, Sutter C, Grail C, Garcia-Marin C, *et al*. Monthly mosquito
857 sampling in Montpellier (Occitanie), France, 2023 [Internet]. IRD - Institute of Research for

Development; 2024 [cited 2025 Mar 6]. Available from: https://www.gbif.org/dataset/8e52f35a-2522-4865-8361-5c249310a7cf

47. Moiroux N. ‘Chapitre 5 : Modélisation spatio-temporelle du contact homme-vecteur’. In: Modélisation du risque d’exposition aux moustiques vecteurs de *Plasmodium* spp dans un contexte de lutte anti-vectorielle" [Internet]. Université Montpellier-II Sciences et Techniques du Languedoc; 2012. p. 76. Available from: https://theses.hal.science/tel-00812118

48. Bartholomée C, Moiroux N. Conceptual model of *Aedes albopictus* in urban environments [Internet]. Zenodo; 2025 [cited 2025 Mar 6]. Available from: https://zenodo.org/doi/10.5281/zenodo.14981760

49. Arduino M de B, Mucci LF, Santos LM dos, Soares MF de S. Importance of microenvironment to arbovirus vector distribution in an urban area, São Paulo, Brazil. Rev Soc Bras Med Trop. 2020;53:e20190504.

50. Neteler M, Roiz D, Rocchini D, Castellani C, Rizzoli A. Terra and Aqua satellites track tiger mosquito invasion: modelling the potential distribution of *Aedes albopictus* in north-eastern Italy. Int J Health Geogr. 2011;10(1):49.

51. Chadwick LE, Williams CM. The effects of atmospheric pressure and composition on the flight of drosophila. Biol Bull. 1949 Oct;97(2):115–37.

52. Pellegrino AC, Peñaflor MFGV, Nardi C, Bezner-Kerr W, Guglielmo CG, Bento JMS, *et al*. Weather forecasting by insects: modified sexual behaviour in response to atmospheric pressure changes. Lazzari CR, editor. PLoS ONE. 2013 Oct 2;8(10):e75004.

53. Haufe WO. The effects of atmospheric pressure on the flight responses of *Aedes aegypti* (L.). Bull Entomol Res. 1954 Sep;45(3):507–26.

880 54. Duque L, Steffan-Dewenter I. Air pollution: a threat to insect pollination. Front Ecol Environ.
881 2024 Apr;22(3):e2701.

882 55. Ryalls JMW, Langford B, Mullinger NJ, Bromfield LM, Nemitz E, Pfrang C, *et al*. Anthropogenic
883 air pollutants reduce insect-mediated pollination services. Environ Pollut. 2022
884 Mar;297:118847.

885 56. Ryalls JMW, Bishop J, Mofikoya AO, Bromfield LM, Nakagawa S, Girling RD. Air pollution
886 disproportionately impairs beneficial invertebrates: a meta-analysis. Nat Commun. 2024 Jul
887 11;15(1):5447.

888 57. Zellweger RM, Cano J, Mangeas M, Taglioni F, Mercier A, Despinoy M, *et al*. Socioeconomic and
889 environmental determinants of dengue transmission in an urban setting: An ecological study in
890 Nouméa, New Caledonia. Messer WB, editor. PLoS Negl Trop Dis. 2017 Apr 3;11(4):e0005471.

891 58. Little E, Biehler D, Leisnham PT, Jordan R, Wilson S, LaDeau SL. Socio-ecological mechanisms
892 supporting high densities of *Aedes albopictus* (Diptera: Culicidae) in Baltimore, MD. J Med
893 Entomol. 2017 Sep 1;54(5):1183–92.

894 59. Rodrigues M de M, Marques GRAM, Serpa LLN, Arduino M de B, Voltolini JC, Barbosa GL, *et al*.
895 Density of *Aedes aegypti* and *Aedes albopictus* and its association with number of residents and
896 meteorological variables in the home environment of dengue endemic area, São Paulo, Brazil.
897 Parasit Vectors. 2015 Dec;8(1):115.

898 60. Moiroux N, Djènontin A, Bio-Bangana AS, Chandre F, Corbel V, Guis H. Spatio-temporal analysis
899 of abundances of three malaria vector species in southern Benin using zero-truncated models.
900 Parasit Vectors. 2014;7(1):103.

61. Taconet P, Porciani A, Soma DD, Mouline K, Simard F, Koffi AA, *et al*. Data-driven and interpretable machine-learning modeling to explore the fine-scale environmental determinants of malaria vectors biting rates in rural Burkina Faso. Parasit Vectors. 2021 Jun 29;14(1):345.

62. Breiman L. Random forest. Mach Learn. 2001;45(1):5–32.

63. Nakagawa S, Schielzeth H. A general and simple method for obtaining R^2 from generalized linear mixed-effects models. O'Hara RB, editor. Methods Ecol Evol. 2013 Feb;4(2):133–42.

64. Curriero FC, Shone SM, Glass GE. Cross Correlation Maps: A tool for visualizing and modeling time lagged associations. Vector-Borne Zoonotic Dis. 2005 Sep;5(3):267–75.

65. Zuur AF, Ieno EN, Elphick CS. A protocol for data exploration to avoid common statistical problems: *Data exploration*. Methods Ecol Evol. 2010 Mar;1(1):3–14.

66. Speiser JL, Miller ME, Tooze J, Ip E. A comparison of random forest variable selection methods for classification prediction modeling. Expert Syst Appl. 2019 Nov;134:93–101.

67. Meyer H, Reudenbach C, Hengl T, Katurji M, Nauss T. Improving performance of spatio-temporal machine learning models using forward feature selection and target-oriented validation. Environ Model Softw. 2018 Mar;101:1–9.

68. Bradley AP. The use of the area under the ROC curve in the evaluation of machine learning algorithms. Pattern Recognit. 1997 Jul;30(7):1145–59.

69. Friedman JH. Greedy function approximation: A gradient boosting machine. Ann Stat [Internet]. 2001 Oct 1 [cited 2024 Aug 29];29(5). Available from: https://projecteuclid.org/journals/annals-of-statistics/volume-29/issue-5/Greedy-function-approximation-A-gradient-boosting-machine/10.1214/aos/1013203451.full

70. R Core Team. R: A language and environment for statistical. R foundation for statistical computing, Vienna, Austria. [Internet]. 2021. Available from: https://www.R-project.org/.

71. Pebesma E. Simple Features for R: standardized support for spatial vector data. R J. 2018;10(1):439.

72. Hijmans RJ. raster: geographic data analysis and modeling [Internet]. 2010 [cited 2024 Aug 29]. p. 3.6-26. Available from: https://CRAN.R-project.org/package=raster

73. Ross N. fasterize: Fast polygon to raster conversion [Internet]. 2018 [cited 2024 Aug 29]. p. 1.0.5. Available from: https://CRAN.R-project.org/package=fasterize

74. Hesselbarth MHK, Sciaini M, Nowosad J, Hanss S. landscapemetrics: Landscape metrics for categorical map patterns [Internet]. 2018 [cited 2024 Aug 29]. p. 2.1.4. Available from: https://CRAN.R-project.org/package=landscapemetrics

75. Brooks M E, Kristensen K, Benthem K J ,van, Magnusson A, Berg C W, Nielsen A, *et al*. glmmTMB balances speed and flexibility among packages for zero-inflated generalized linear mixed modeling. R J. 2017;9(2):378.

76. Lüdecke D, Ben-Shachar M, Patil I, Waggoner P, Makowski D. performance: An R package for assessment, comparison and testing of statistical models. J Open Source Softw. 2021 Apr 21;6(60):3139.

77. Makowski D, Ben-Shachar M, Patil I, Lüdecke D. Methods and algorithms for correlation analysis in R. J Open Source Softw. 2020 Jul 16;5(51):2306.

78. Kuhn M. Building predictive models in *R* using the **caret** Package. J Stat Softw [Internet]. 2008 [cited 2024 Jun 6];28(5). Available from: http://www.jstatsoft.org/v28/i05/

79. Wright MN, Ziegler A. **ranger** : A fast Implementation of Random Forests for high gimensional gata in *C++* and *R*. J Stat Softw [Internet]. 2017 [cited 2024 Jun 6];77(1). Available from: http://www.jstatsoft.org/v77/i01/

80. Meyer H, Ludwig M, Milà C, Linnenbrink J, Schumacher F. The CAST package for training and assessment of spatial prediction models in R [Internet]. arXiv; 2024 [cited 2025 Jan 8]. Available from: https://arxiv.org/abs/2404.06978

81. Molnar C. iml: An R package for interpretable machine learning. J Open Source Softw. 2018 Jun 27;3(26):786.

82. Greenwell B M. pdp: An R package for constructing partial dependence plots. R J. 2017;9(1):421.

83. Yan Y. MLmetrics: machine learning evaluation metrics [Internet]. 2015 [cited 2025 Jan 8]. p. 1.1.3. Available from: https://CRAN.R-project.org/package=MLmetrics

84. Saito T, Rehmsmeier M. Precrec: fast and accurate precision–recall and ROC curve calculations in R. Wren J, editor. Bioinformatics. 2017 Jan 1;33(1):145–7.

85. Pedersen TL. patchwork: The Composer of Plots [Internet]. 2019 [cited 2025 Jan 8]. p. 1.3.0. Available from: https://CRAN.R-project.org/package=patchwork

86. Benito B. BlasBenito/spatialRF: spatialRF: Easy spatial regression with random forest [Internet]. Zenodo; 2021 [cited 2025 Jan 8]. Available from: https://zenodo.org/record/4745208

87. Taconet P, Bartholomée C. R scripts to reproduce the analysis of the publication 'Investigating the role of urban vegetation alongside other environmental variables in shaping *Aedes albopictus* presence and abundance in Montpellier, France' [Internet]. [cited 2025 Mar 11]. Available from: https://archive.softwareheritage.org/browse/directory/76ee4af2ae1786fe1808f74bdcd7f676

8aecf4ef/?origin_url=https://github.com/ptaconet/modeling_vector_mtp&revision=2865eca51e7b85a87d60ee43aa05829f097256a1&snapshot=47732a56dff624a2105d486e6ed98c6a7b64d3e2

88. Honório NA, Castro MG, Barros FSM de, Magalhães M de AFM, Sabroza PC. The spatial distribution of *Aedes aegypti* and *Aedes albopictus* in a transition zone, Rio de Janeiro, Brazil. Cad Saúde Pública. 2009 Jun;25(6):1203–14.

89. Sun H, Dickens BL, Richards D, Ong J, Rajarethinam J, Hassim MEE, *et al*. Spatio-temporal analysis of the main dengue vector populations in Singapore. Parasit Vectors. 2021 Dec;14(1):41.

90. Knop E, Grimm ML, Korner-Nievergelt F, Schmid B, Liechti F. Patterns of high-flying insect abundance are shaped by landscape type and abiotic conditions. Sci Rep. 2023 Sep 13;13(1):15114.

91. Keefe HE, Kharouba HM. Growing degree-days do not explain moth species' distributions at broad scales. Ecosphere. 2024 Jul;15(7):e4885.

92. Reinhold J, Lazzari C, Lahondère C. Effects of the Environmental Temperature on *Aedes aegypt*i and *Aedes albopictus* Mosquitoes: A Review. Insects. 2018 Nov 6;9(4):158.

93. Jourdain F, Roiz D, de Valk H, Noël H, L'Ambert G, Franke F, *et al*. From importation to autochthonous transmission: Drivers of chikungunya and dengue emergence in a temperate area. Lambrechts L, editor. PLoS Negl Trop Dis. 2020 May 11;14(5):e0008320.

94. Le Goff G, Damiens D, Ruttee AH, Jean F, Payet L, Lebon C, *et al*. Spatial and temporal characterization of *Aedes albopictus* oviposition activity in candidate urban settings for sterile insect technique testing in La Reunion Island. Infect Dis Poverty. 2024 Oct 25;13(1):78.

95. Adeleke ED, Shittu RA, Beierkuhnlein C, Thomas SM. High wind speed prevents the establishment of the disease vector mosquito *Aedes albopictus* in its climatic niche in Europe. Front Environ Sci. 2022 Jun 8;10:846243.

96. Afriyanie D, Akbar R, Suroso DSA. Socio-ecological resilience for urban green space allocation. IOP Conf Ser Earth Environ Sci. 2018 Apr;145:012120.

97. Paudel S, States SL. Urban green spaces and sustainability: Exploring the ecosystem services and disservices of grassy lawns versus floral meadows. Urban For Urban Green. 2023 Jun;84:127932.

98. Menconi ME, Palazzoni L, Grohmann D. Core themes for an urban green systems thinker: A review of complexity management in provisioning cultural ecosystem services. Urban For Urban Green. 2021 Nov;65:127355.

99. Smith DL, Perkins TA, Tusting LS, Scott TW, Lindsay SW. Mosquito population regulation and larval source management in heterogeneous environments. Vasilakis N, editor. PLoS ONE. 2013 Aug 7;8(8):e71247.

100. Tredennick AT, Hooker G, Ellner SP, Adler PB. A practical guide to selecting models for exploration, inference, and prediction in ecology. Ecology. 2021 Jun;102(6):e03336.

101. Tran A, Biteau-Coroller F, Guis H. Modelisation des maladies vectorielles. 2005;

102. Foudriat M. La co-construction [Internet]. 2éd. Presses de l'EHESP; 2019 [cited 2025 Feb 27]. Available from: http://www.cairn.info/la-co-construction--9782810908257.htm

103. Kapp R. City of Stuttgart and green and blue space adaptation for urban areas and eco towns (GRaBS) [Internet]. 2022 [cited 2024 Oct 11]. Available from: https://climate-adapt.eea.europa.eu/fr/metadata/case-studies/stuttgart-combating-the-heat-island-effect-and-poor-air-quality-with-green-ventilation-corridors

104. Conseil des Architectes d'Europe. Corridor vert de Lisbonne [Internet]. [cited 2024 Oct 11]. Available from: https://www.ace-cae.eu/fr/activites/projets-europeens/projets-termines/connectarch/20-projets-architecturaux-contre-le-changement-climatique/corridor-vert-de-lisbonne/

Supporting informations

S1 Table: Table with sampling areas characterization.

S2 Table: Summary of the different variables used, with their processing, acquisition methods or source database and temporal/spatial scale.

S3 Table: Description of the landscape metrics for each landscape class for each trap, by buffer.

S4 Table: Mosquito density/trap/24h by species and sex in the nine different sampling areas. The mosquito density represents the marginal mean of the number of mosquitoes caught per trap per 24 hours, calculated based on the sampling environment, with the standard error specified (SE).

S5 Table: Variables Selected After Bivariate Analyses, with Justifications for Exclusion from Multivariate Analysis (Correlation, VIF, Recursive Feature Elimination)

1032 **S1 Fig: BG-PRO trap on the field and pictures of studied areas.** S1A Fig represents a BG-Pro
1033 on the field, S1B Fig the Park of Aiguelongue, S1C the Botanical Garden, S1D The Bouisson
1034 Bertrand Institute and 1E the Acapulco Hostel.
1035
1036 **S2 Fig: Analysis workflow: from the data acquisition to the multivariate analysis**
1037
1038 **S3 Fig: Time series of weekly cumulated precipitations (1A), mean (TMEAN), minimum**
1039 **(TMIN) and maximum (TMAX) temperature, (1B), growing degree-days (1B), mean relative**
1040 **humidity (1C), mean wind speed (1D) and mean (Patmean), minimum (Patmin) and**
1041 **maximum atmospheric pressure (Patmax), during the studing period.** Vertical dotted red
1042 lines indicate monthly mosquito sampling sessions.
1043
1044 **S4 Fig: Number of *Ae. albopictus* per trap per 24h during the study period, by sampling**
1045 **environment.** Boxes represent medians and interquartile ranges, whiskers indicate minimum
1046 and maximum values, and points show the abundance for each sampling session and day, for
1047 each trap, within the three environments.
1048
1049 **S5 Fig: Cross correlation maps showing the lagged effect of air-quality variables on *Ae.***
1050 ***albopictus* presence or abundance**. Lagged air-quality variables include daily concentration of
1051 nitrogen monoxide (NO), of nitrogen dioxide (NO2), of particulate matter (PM10, PM2.5) and
1052 of ozone (O3). Time lags are expressed in weeks prior to sampling. The adjusted marginal R^2
1053 reflects the variance explained by the explanatory variable, adjusted for correlation direction.
1054 Red-bordered squares highlight the time lag with the highest marginal R^2, with the interval

indicated in the top left corner. Black-bordered squares denote marginal R^2 values close to the highest (within 10%). Gray squares represent correlations with p-values > 0.2.

S6 Fig: Bivariate relationships between *Ae. albopictus* presence or abundance and the sampling environment and the socio-demographic variables. The adjusted marginal R^2 reflects the variance explained by the explanatory variable, adjusted for correlation direction. Boxes are colored if the p-value was < 0.2 (No asterisk: p-value ∈ [0.05; 0.2], *: p-value ∈ [0.01, 0.05], **: p-value ∈ [0.001; 0.01]; ***: p-value ∈ [0; 0.001]). Box color depend on the direction of the relationship (blue : negative, red : positive). Color intensity vary according to the marginal R^2 value.

S7 Fig: Evaluation of presence model. S7A Fig is the Receiver Operating Characteristics (ROC) Curve for the presence model. It illustrates the model's sensitivity (its ability to predict the presence of *Ae. albopictus*) against 1 - Specificity (its ability to detect the absence of *Ae. albopictus*). The Area Under the Curve (AUC) represents the model's ability to discriminate between the presence and absence of the mosquito, with values ranging from 0 to 1. The closer the AUC is to 1, the better the model's predictive performance. S7A Fig shows that the model demonstrated good predictive accuracy, with an AUC of 0.89. S7B Fig compares the observed (in green) versus predicted presence probabilities for each out-of-sample leave-area (yellow) and for each out-of-sample leave-sampling-session (in blue) . The y-axis represents the probability of *Ae. albopictus* presence, while the x-axis corresponds to the sampling session. Figure 10B indicates that the model accurately predicted the spatiotemporal trends of presence/absence, although it tended to overestimate presence.

S8 Fig: Evaluation of abundance model. S8A Fig is a violin plot showing the distribution of residuals for the abundance model. The black dots indicate the median values. The Mean Absolute Error (MAE) and the number of observations (n) are displayed in a square above the plot. This figure demonstrates that the model tends to overestimate low counts of *Aedes albopictus* (fewer than three caught in 24 hours per trap), accurately estimates counts between 4 and 20, and underestimates higher counts (more than 20). S8B Fig compares the observed versus predicted numbers of *Ae. albopictus* caught per site per sampling session (in green), versus predicted numbers for each out-of-sample leave-area (yellow) and for each out-of-sample leave-sampling-session (in blue). The y-axis represents the mean number of d *Ae. albopictus* females caught per trap per area per sampling session, while the x-axis represents the sampling session. This figure confirms the observations made in S8A Fig.

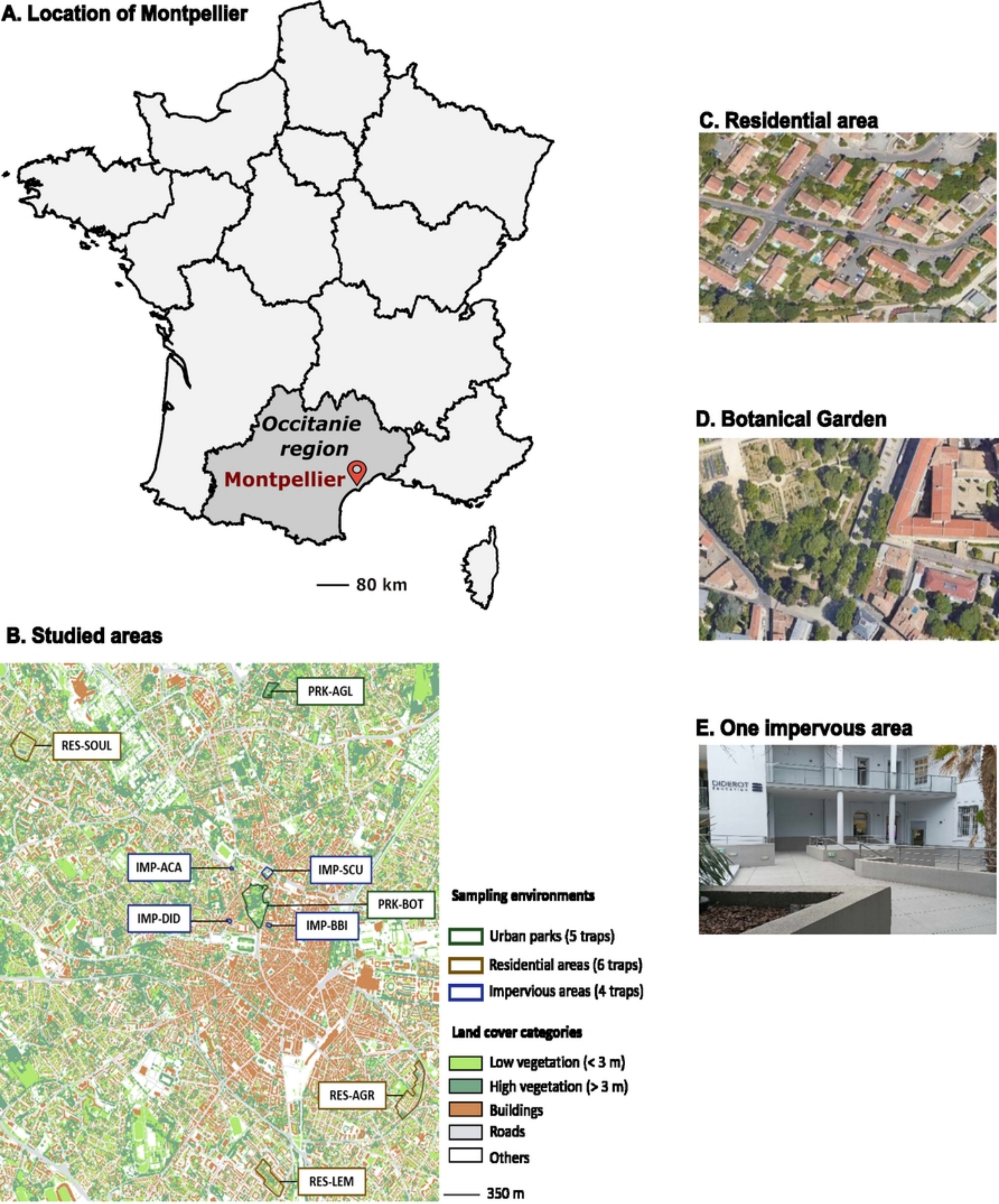
A. Location of Montpellier
Occitanie region
Montpellier
80 km
C. Residential area
D. Botanical Garden
B. Studied areas
PRK-AGL
RES-SOUL
IMP-ACA
IMP-SCU
PRK-BOT
IMP-DID
IMP-BBI
RES-AGR
RES-LEM
Sampling environments
Urban parks (5 traps)
Residential areas (6 traps)
Impervious areas (4 traps)
Land cover categories
Low vegetation (< 3 m)
High vegetation (> 3 m)
Buildings
Roads
Others
350 m
E. One impervous area
DIDEROT

Fig1

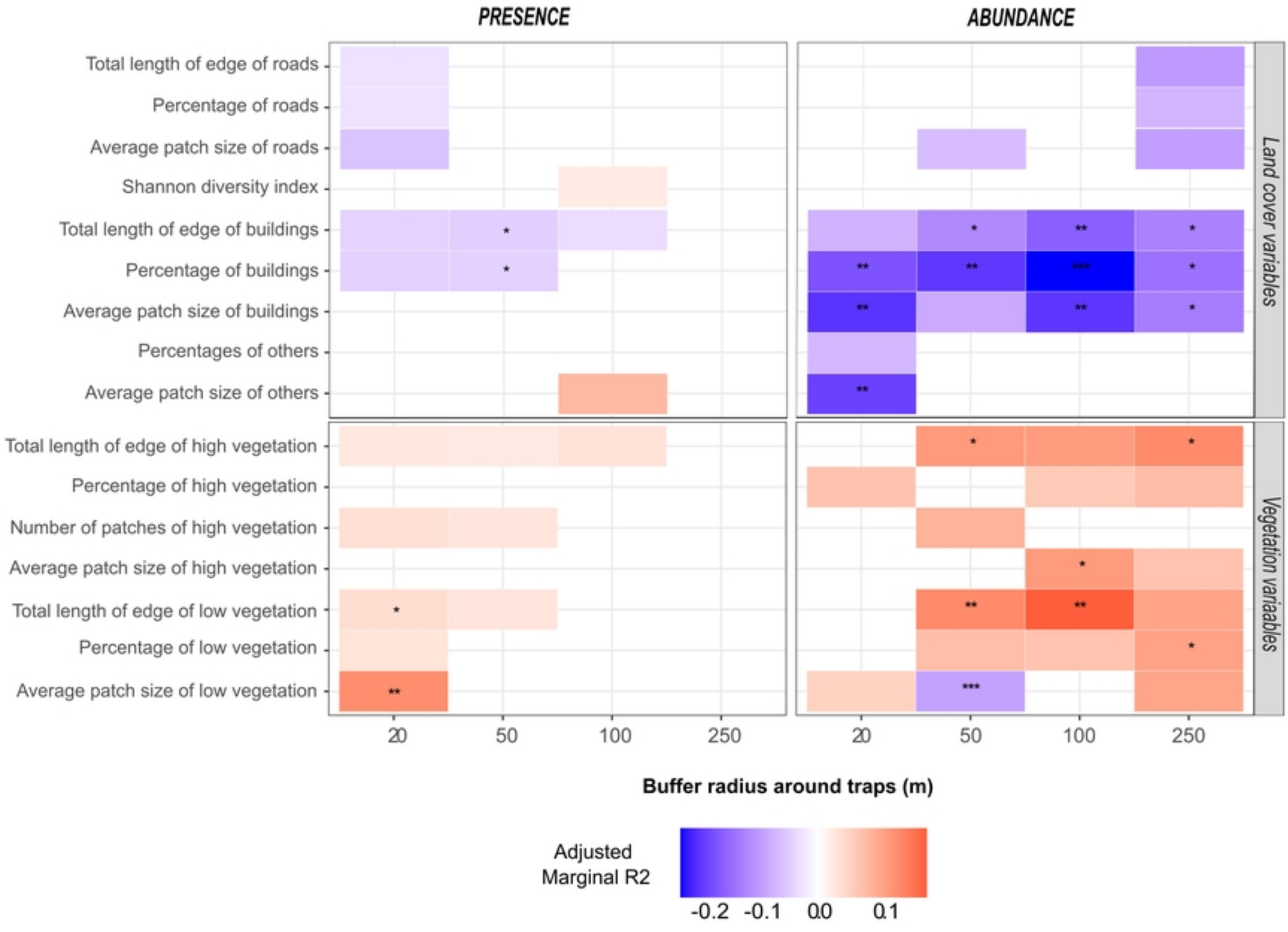
PRESENCE
ABUNDANCE
Total length of edge of roads
Percentage of roads
Average patch size of roads
Shannon diversity index
Total length of edge of buildings
Percentage of buildings
Average patch size of buildings
Percentages of others
Average patch size of others
Total length of edge of high vegetation
Percentage of high vegetation
Number of patches of high vegetation
Average patch size of high vegetation
Total length of edge of low vegetation
Percentage of low vegetation
Average patch size of low vegetation
Land cover variables
Vegetation variables
20
50
100
250
Buffer radius around traps (m)
Adjusted
Marginal R2
-0.2
-0.1
0.0
0.1

Fig2

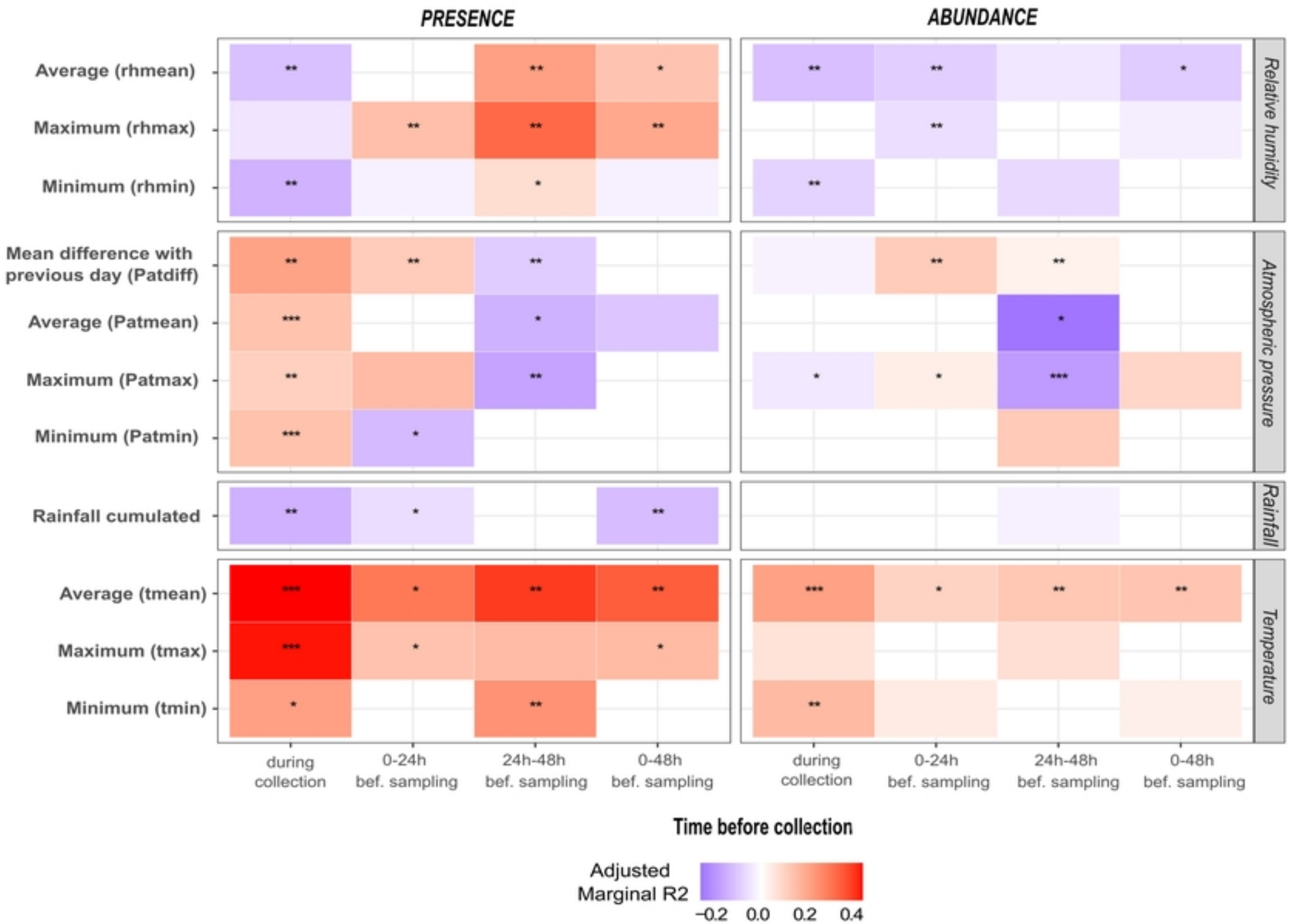
PRESENCE
ABUNDANCE
Average (rhmean)
Maximum (rhmax)
Minimum (rhmin)
Mean difference with previous day (Patdiff)
Average (Patmean)
Maximum (Patmax)
Minimum (Patmin)
Rainfall cumulated
Average (tmean)
Maximum (tmax)
Minimum (tmin)
Relative humidity
Atmospheric pressure
Rainfall
Temperature
during collection
0-24h bef. sampling
24h-48h bef. sampling
0-48h bef. sampling
Time before collection
Adjusted Marginal R2
−0.2
0.0
0.2
0.4

Fig3

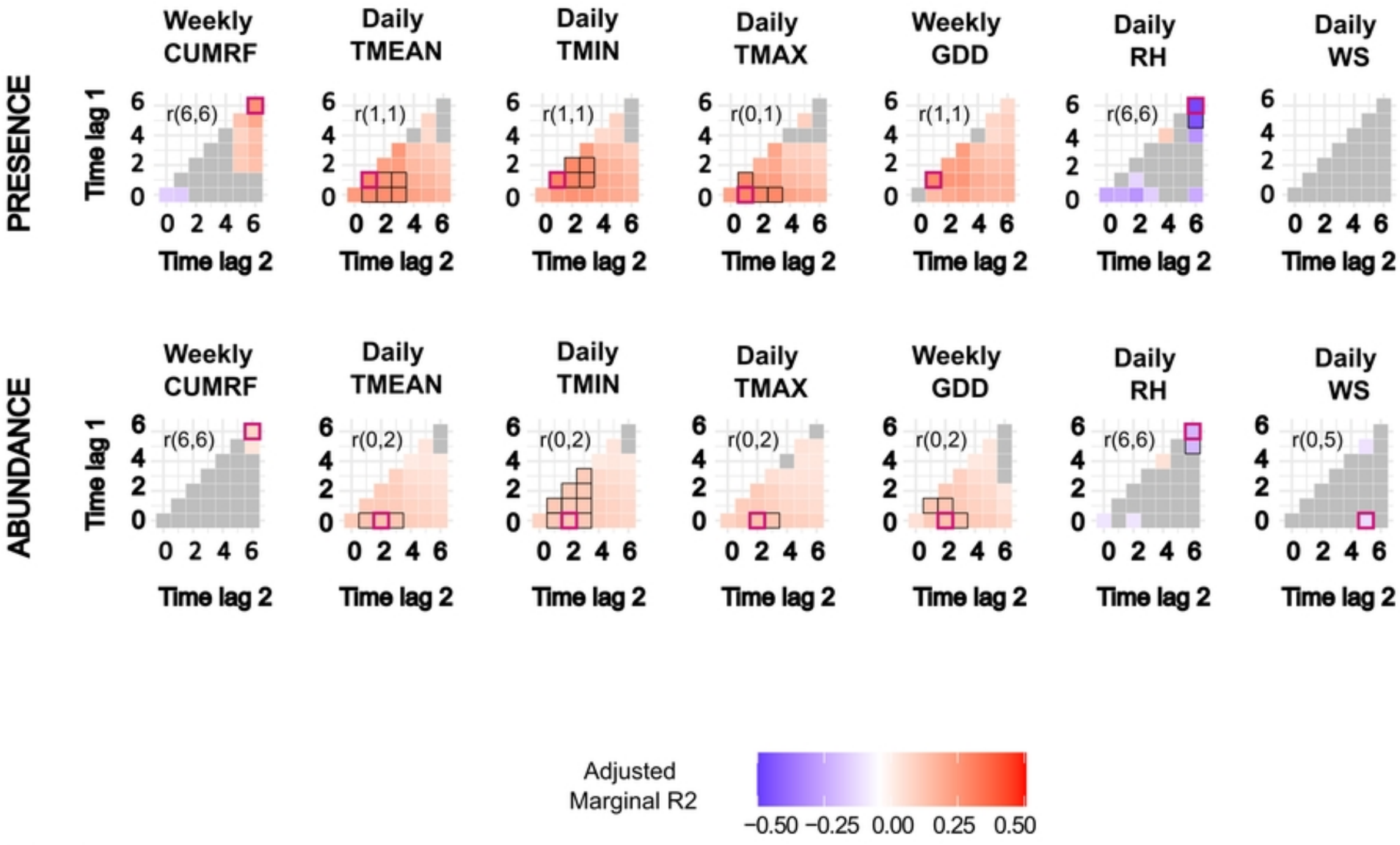
PRESENCE
ABUNDANCE
Weekly CUMRF
Daily TMEAN
Daily TMIN
Daily TMAX
Weekly GDD
Daily RH
Daily WS
Time lag 1
Time lag 2
r(6,6)
r(1,1)
r(1,1)
r(0,1)
r(1,1)
r(6,6)
r(6,6)
r(0,2)
r(0,2)
r(0,2)
r(0,2)
r(6,6)
r(0,5)
Adjusted Marginal R2
−0.50 −0.25 0.00 0.25 0.50

Fig4

A. Variable importance plot

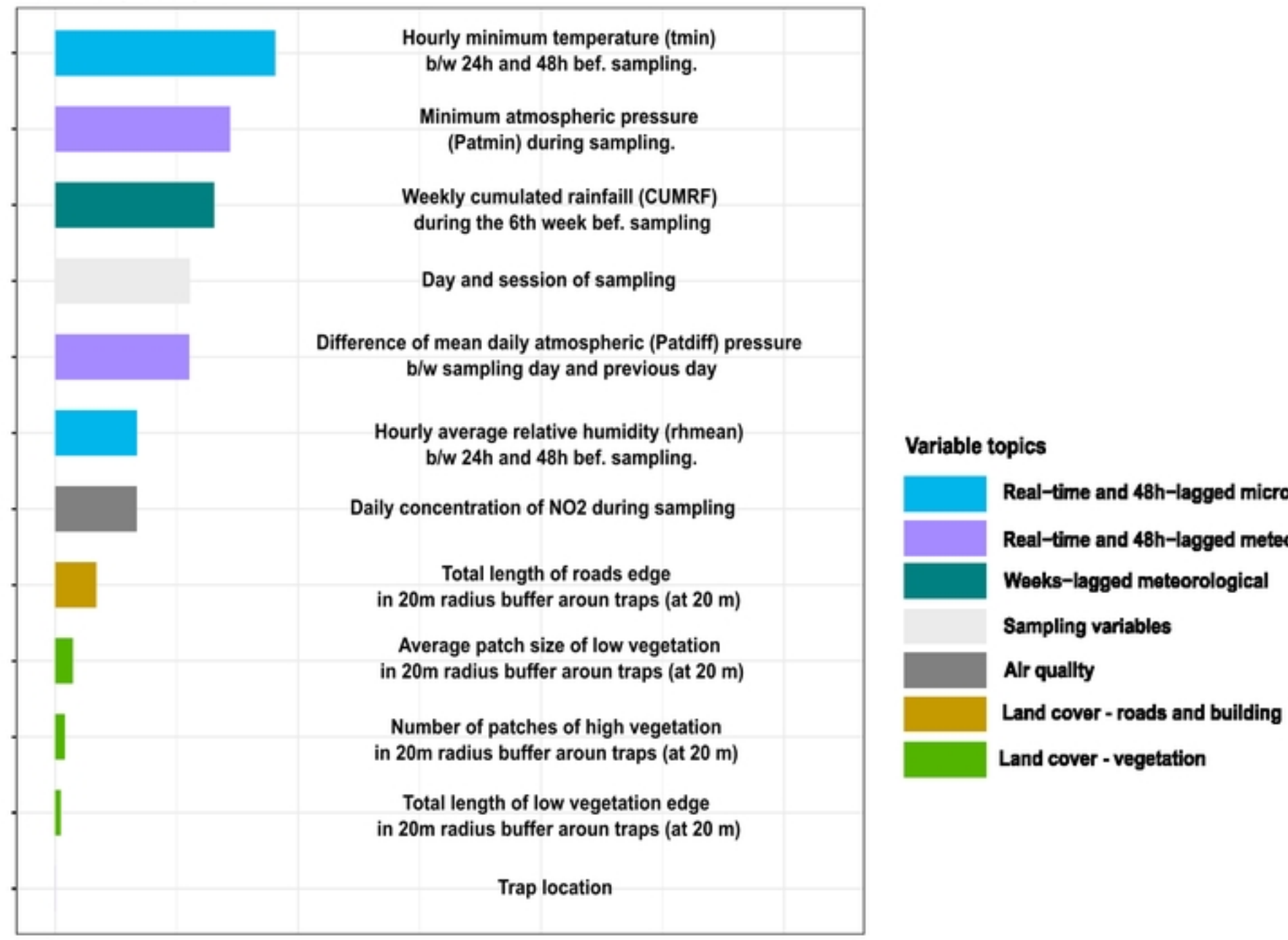

B. Partial Dependence Plots

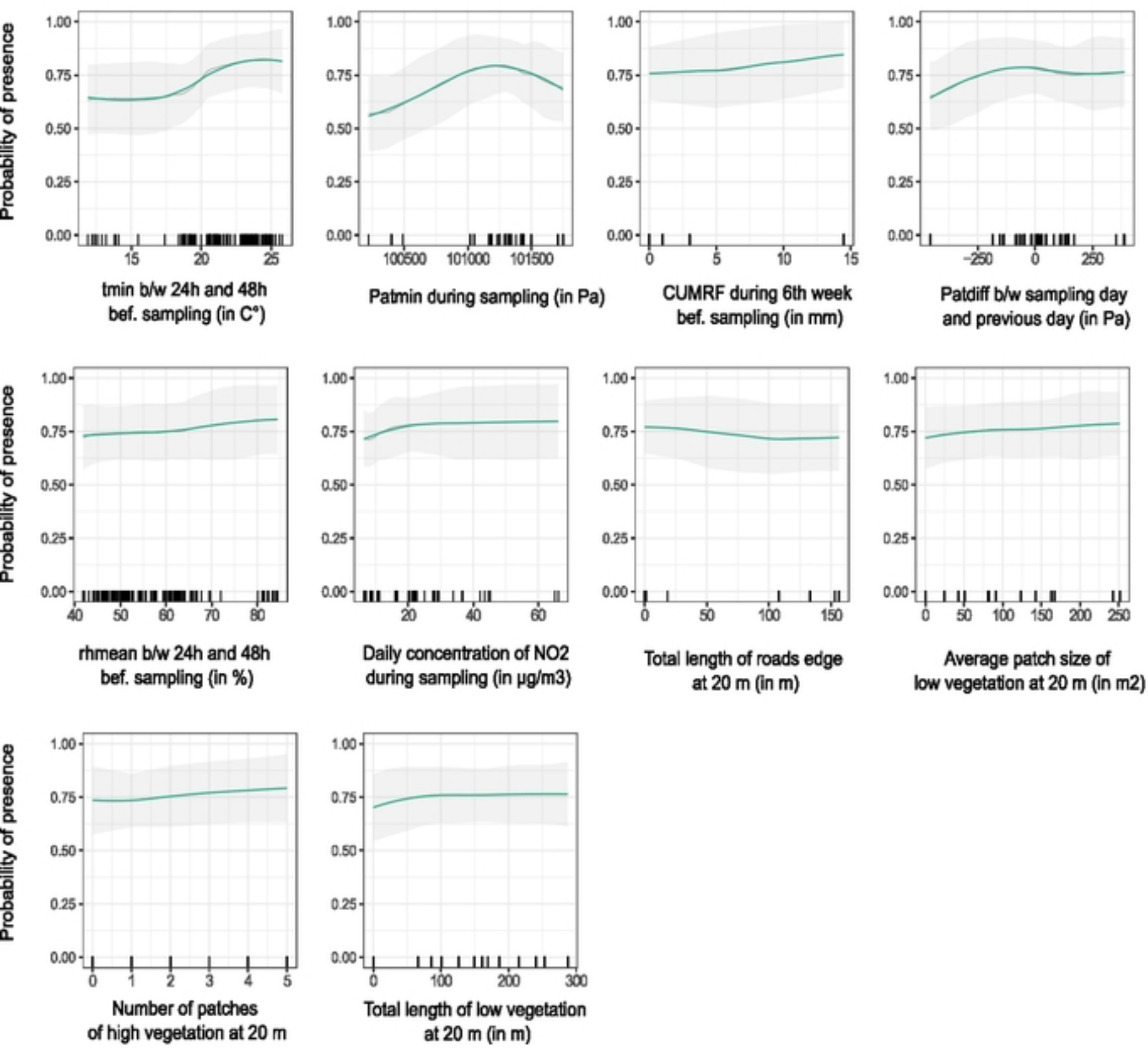

Fig5

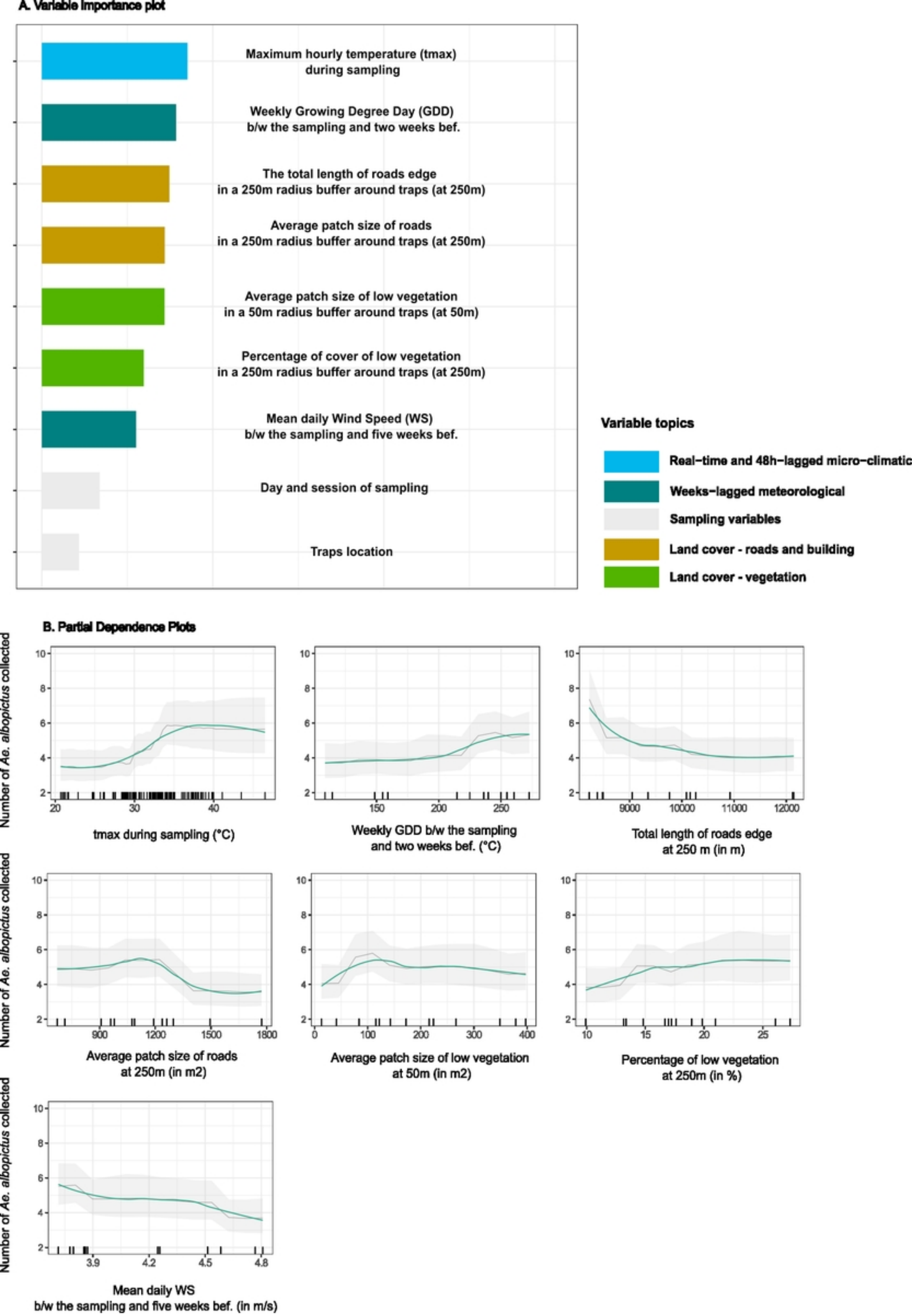
A. Variable importance plot
Maximum hourly temperature (tmax) during sampling
Weekly Growing Degree Day (GDD) b/w the sampling and two weeks bef.
The total length of roads edge in a 250m radius buffer around traps (at 250m)
Average patch size of roads in a 250m radius buffer around traps (at 250m)
Average patch size of low vegetation in a 50m radius buffer around traps (at 50m)
Percentage of cover of low vegetation in a 250m radius buffer around traps (at 250m)
Mean daily Wind Speed (WS) b/w the sampling and five weeks bef.
Day and session of sampling
Traps location
Variable topics
Real-time and 48h-lagged micro-climatic
Weeks-lagged meteorological
Sampling variables
Land cover - roads and building
Land cover - vegetation
B. Partial Dependence Plots
Number of Ae. albopictus collected
tmax during sampling (°C)
Weekly GDD b/w the sampling and two weeks bef. (°C)
Total length of roads edge at 250 m (in m)
Average patch size of roads at 250m (in m2)
Average patch size of low vegetation at 50m (in m2)
Percentage of low vegetation at 250m (in %)
Mean daily WS b/w the sampling and five weeks bef. (in m/s)

Fig6